

Relaxed constraints on the heavy scalar masses in 2HDM

Siddhartha Karmakar^{*} and Subhendu Rakshit[†]

*Discipline of Physics, Indian Institute of Technology Indore,
Khandwa Road, Simrol, Indore - 453 552, India*

Abstract

In the wake of new scalar searches at LHC in various channels, it is interesting to investigate the sacrosanctity of the constraints on the masses and couplings of the heavier scalars in a two-Higgs-doublet model (2HDM). We consider the effects of new physics beyond a 2HDM encoded in terms of bosonic dim-6 operators. Although these constraints are mostly immune to such new physics, we demonstrate for a specific class of bosonic operators, the constraints on the masses of the exotic scalars from cascade decays can get substantially relaxed. We present such effects for both degenerate and hierarchical mass spectra of the heavier scalars in 2HDM. Some decay channels of the new scalars vanish at the alignment limit in the tree-level 2HDM. But the inclusion of dim-6 terms can lead to significant cross-sections for such processes. It is also pointed out that observation of such processes can no longer rule out the alignment limit if such dim-6 operators are present.

^{*} E-mail: phd1401251010@iiti.ac.in

[†] E-mail: rakshit@iiti.ac.in

I. INTRODUCTION

Even after the discovery of a Higgs boson [1, 2] whose characteristics resemble that of the standard model (SM) Higgs, the dynamics of electroweak symmetry breaking and the structure of the scalar sector remains an open question. The non-cancellation of quadratic divergence of Higgs mass under the framework of SM has motivated plethora of beyond-standard model (BSM) theories for decades. The two-Higgs-doublet model (2HDM) is an archetype of an extended scalar sector, theoretically well-motivated from the viewpoint of supersymmetry, composite Higgs models, etc. For example, in supersymmetric models [3] the motivation behind a second Higgs doublet is twofold: firstly to cancel chiral anomalies created by the superpartners of such scalars, and secondly from the requirement of the superpotential to be holomorphic. 2HDMs arising in the framework of composite Higgs [4], Little Higgs [5], Twin Higgs [6] have also been studied in the literature. Even keeping the hierarchy problem aside, it is often deployed to explain issues of electroweak baryogenesis [7], flavour anomalies [8], neutrino mass [9], dark matter [10], etc.

In light of measurements of the signal strengths of the observed Higgs, any model with a scalar sector beyond the SM must contain a CP-even neutral scalar whose couplings are aligned to that of the SM Higgs boson. Such an alignment can be realised when the new scalars which mix with the SM-like Higgs, are decoupled from the mass spectrum of SM *à la* Applequist-Carrazone [11, 12]. The ‘alignment without decoupling’ scenario becomes viable only for models with additional scalar doublets [12–18]. In such cases, the scalars can have masses below a TeV, *i.e.*, well within the reach of LHC. Thus, along with the signal strengths of the SM-like Higgs, the direct bounds on the masses of exotic scalars also play a pivotal role in constraining the parameter space of 2HDM. Such bounds also depend on the specifications of the Yukawa sector of the models. Non-observation of such new scalars rule out a significant region of parameter space in the ‘alignment without decoupling’ scenarios. Also, some decay channels involving exotic scalars remain absent at the alignment limit in a CP-conserving 2HDM [19]. If the LHC discovers any new scalar state in one of these channels, the interpretation involving a CP-conserving 2HDM would readily imply a deviation from the alignment limit.

If new physics beyond 2HDM exists as a decoupled sector from the mass scale of 2HDM,

the effects of such new physics can be encoded in the higher-dimensional operators in an effective theory where the fields of 2HDM constitute the low-energy spectrum [20–22]. Such an effective theory is dubbed as two-Higgs-doublet model effective field theory (2HDMEFT) in the literature. Several aspects of such effective theories for various extended scalar sectors have been addressed in the literature [23–27]. A complete basis of the 6-dim operators in 2HDMEFT has been introduced only recently [22]. It has also been shown that such 6-dim operators are capable of masking the true alignment limit in a 2HDM, by modifying various decay channels of the SM-like Higgs boson [28]. In the present paper, we have investigated the role of such 6-dim terms while extracting the LHC constraints on the masses of the new scalars in a 2HDM. We consider different mass spectra of these new scalars allowed from the theoretical constraints and measurements of the oblique parameters. The constraints ensuing from different searches for the heavy scalars at the LHC and possible deviations in the presence of 6-dim terms have been illustrated.

In Sec. II we briefly review the theoretical framework of a general 2HDM. In Sec. III we discuss the theoretical as well as phenomenological constraints on the parameter space of a 2HDM relevant to this work. In Sec. IV we introduce the 6-dim terms that have been considered in this work, along with the modified couplings of the scalars. In Sec. V we present the benchmark scenarios to illustrate the effect of such 6-dim terms on the parameter space of the 2HDM and eventually conclude in Sec. VI.

II. 2HDM: A REVIEW

The two scalar doublets are defined as:

$$\varphi_I = \begin{pmatrix} \phi_I^+ \\ \frac{1}{\sqrt{2}}(v_I + \rho_I) + i\eta_I \end{pmatrix}, \quad (2.1)$$

with $I = 1, 2$. Here ϕ_I^\pm , ρ_I , η_I , and v_I denote the charged, neutral CP-even and neutral CP-odd degrees of freedom (d.o.f.) and the vacuum expectation value (vev) of the I -th doublet respectively.

Before spontaneous symmetry breaking (SSB), the tree-level 2HDM Lagrangian, augmented with 6-dim operators, assumes the form

$$\mathcal{L} = \mathcal{L}_{kin} + \mathcal{L}_{Yuk} - V(\varphi_1, \varphi_2) + \mathcal{L}_6, \quad (2.2)$$

where,

$$\begin{aligned}
\mathcal{L}_{kin} &= -\frac{1}{4} \sum_{X=G^a, W^i, B} X_{\mu\nu} X^{\mu\nu} + \sum_{I=1,2} |D_\mu \varphi_I|^2 + \sum_{\psi=Q, L, u, d, l} \bar{\psi} i \not{D} \psi, \\
\mathcal{L}_{Yuk} &= \sum_{I=1,2} Y_I^e \bar{l} e \varphi_I + \sum_{I=1,2} Y_I^d \bar{q} d \varphi_I + \sum_{I=1,2} Y_I^u \bar{q} u \tilde{\varphi}_I, \\
V(\varphi_1, \varphi_2) &= m_{11}^2 |\varphi_1|^2 + m_{22}^2 |\varphi_2|^2 - (\mu^2 \varphi_1^\dagger \varphi_2 + h.c.) + \lambda_1 |\varphi_1|^4 + \lambda_2 |\varphi_2|^4 + \lambda_3 |\varphi_1|^2 |\varphi_2|^2 \\
&\quad + \lambda_4 |\varphi_1^\dagger \varphi_2|^2 + \left[\left(\frac{\lambda_5}{2} \varphi_1^\dagger \varphi_2 + \lambda_6 |\varphi_1|^2 + \lambda_7 |\varphi_2|^2 \right) \varphi_1^\dagger \varphi_2 + h.c. \right], \\
\mathcal{L}_6 &= \sum_i c_i O_i / f^2.
\end{aligned} \tag{2.3}$$

Here, c_i is the Wilson coefficient of the 6-dim operator O_i and f is the scale of new physics beyond the tree-level 2HDM. The terms proportional to $\lambda_{6,7}$ are called ‘hard- Z_2 violating’ because they lead to a quadratically divergent amplitude for $\varphi_1 \leftrightarrow \varphi_2$ transition [29] and they also lead to CP-violation in the scalar sector [30]. But it is possible to realise the CP-conserving limit with non-zero values of $\lambda_{6,7}$ as well [19]. In this paper we contain our discussion to the CP-conserving 2HDM, and we take $\lambda_{6,7} = 0$. The electroweak symmetry is broken by the vacuum expectation values (vev), namely v_1 and v_2 corresponding to the two doublets $\varphi_{1,2}$ respectively. This leads to the mixing of similar types of degrees of freedom pertaining to $\varphi_{1,2}$. In the CP-conserving case, the mass matrices of the neutral CP-even and odd scalars and the charged scalars are diagonalised by the following field rotations:

$$\begin{pmatrix} H \\ h \end{pmatrix} = R(\alpha) \begin{pmatrix} \rho_1 \\ \rho_2 \end{pmatrix}, \quad \begin{pmatrix} W_L^\pm \\ H^\pm \end{pmatrix} = R(\beta) \begin{pmatrix} \phi_1^\pm \\ \phi_2^\pm \end{pmatrix}, \quad \begin{pmatrix} Z_L \\ A \end{pmatrix} = R(\beta) \begin{pmatrix} \eta_1 \\ \eta_2 \end{pmatrix}. \tag{2.4}$$

Here,

$$R(\theta) = \begin{bmatrix} \cos \theta & \sin \theta \\ -\sin \theta & \cos \theta \end{bmatrix}. \tag{2.5}$$

h, H are the neutral CP-even physical d.o.f., whereas A and H^\pm are the neutral CP-odd and charged d.o.f respectively. As it can be seen from eq. (2.4), β is the mixing angle of the charged and CP-odd sectors and it is given by $\beta = \tan^{-1}(v_2/v_1)$. α is the mixing angle of the CP-even neutral scalars and can be expressed as

$$\alpha = \sin^{-1} \left[\frac{\mathcal{M}_{\rho 12}^2}{\sqrt{(\mathcal{M}_{\rho 12}^2)^2 + (\mathcal{M}_{\rho 11}^2 - m_h^2)^2}} \right], \tag{2.6}$$

with \mathcal{M}_ρ^2 being the mass-squared matrix in the neutral CP-even sector. In this paper, we assume h to be the SM-like Higgs with a mass of $m_h \sim 125.09$ GeV and $m_H > m_h$. The case of $m_H < m_h$ has been explored in the literature as well [16]. It was shown that the tree-level Higgs-mediated flavour-changing neutral currents (FCNC) appear in models where more than one scalar doublet give mass to the same kind of SM fermions [31, 32]. Such a situation can be avoided under the framework of various discrete symmetries, for example, a Z_2 symmetry [31, 32]. There are four possible ways in which such a Z_2 charge assignment of the SM fermions can be done, namely the type-I ($Y_1^u = Y_1^d = Y_1^e = 0$), type-II ($Y_1^u = Y_2^d = Y_2^e = 0$), type-III ($Y_1^u = Y_2^d = Y_1^e = 0$) and type-IV ($Y_1^u = Y_1^d = Y_2^e = 0$) cases. Type-II scenario is also dubbed as the MSSM-like case due to similarity in the Yukawa sectors. Type-III and -IV are sometimes also referred to as flipped and lepton-specific scenarios respectively. Due to the rotation in the scalar sector following eq. (2.4), the couplings of the SM gauge bosons and fermions to the SM-like Higgs boson are rescaled compared to the corresponding SM values. After SSB the Yukawa sector of the 2HDM can be written as,

$$\begin{aligned}
-\mathcal{L}_{Yuk} = & \frac{1}{\sqrt{2}}(\kappa_D s_{\beta-\alpha} + \rho_D c_{\beta-\alpha})\bar{D}Dh + \frac{1}{\sqrt{2}}(\kappa_D c_{\beta-\alpha} - \rho_D s_{\beta-\alpha})\bar{D}DH \\
& + \frac{1}{\sqrt{2}}(\kappa_U s_{\beta-\alpha} + \rho_U c_{\beta-\alpha})\bar{U}Uh + \frac{1}{\sqrt{2}}(\kappa_U c_{\beta-\alpha} - \rho_U s_{\beta-\alpha})\bar{U}UH \\
& + \frac{1}{\sqrt{2}}(\kappa_L s_{\beta-\alpha} - \rho_L c_{\beta-\alpha})\bar{L}Lh + \frac{1}{\sqrt{2}}(\kappa_L c_{\beta-\alpha} - \rho_L s_{\beta-\alpha})\bar{L}LH \\
& - \frac{i}{\sqrt{2}}\bar{U}\gamma_5\rho_U UA + \frac{i}{\sqrt{2}}\bar{D}\gamma_5\rho_D DA + \frac{i}{\sqrt{2}}\bar{L}\gamma_5\rho_L LA \\
& + \left(\bar{U}(V_{CKM}\rho_DP_R - \rho_U V_{CKM}P_L)DH^+ + \bar{\nu}\rho_LP_R LH^+ + \text{h.c.}\right), \tag{2.7}
\end{aligned}$$

with, $\kappa_f = \sqrt{2}M_f/v$ for $f = U, D, L$ and,

	Type-I	Type-II	Type-III	Type-IV
ρ_D	$\kappa_D \cot \beta$	$-\kappa_D \tan \beta$	$-\kappa_D \tan \beta$	$\kappa_D \cot \beta$
ρ_U	$\kappa_U \cot \beta$	$\kappa_U \cot \beta$	$\kappa_U \cot \beta$	$\kappa_U \cot \beta$
ρ_L	$\kappa_L \cot \beta$	$-\kappa_L \tan \beta$	$\kappa_L \cot \beta$	$-\kappa_L \tan \beta$.

U, D, L and ν represent the up-type, down-type quarks, charged leptons and neutrinos in their mass bases respectively. The generation indices of the fermionic fields have been suppressed in eq. (2.7). As mentioned earlier, the measurement of the signal strengths of the SM-like Higgs at LHC demands that the properties of one of the neutral CP-even neutral

scalars, here h , should closely resemble to that of the SM Higgs. As eq. (2.7) indicates, this is satisfied near the so-called ‘alignment limit’, *i.e.*, $\cos(\beta - \alpha) \rightarrow 0$. The measurement of the Higgs signal strengths dictate that for type-II 2HDM, at $\tan \beta \sim 1$, the constraint on $\cos(\beta - \alpha)$ is given by $-0.05 \lesssim \cos(\beta - \alpha) \lesssim 0.15$ at 95% CL. The allowed region becomes even smaller for higher values of $\tan \beta$. Such a constraint is comparably relaxed in type-I 2HDM, where the allowed range is $|\cos(\beta - \alpha)| \lesssim 0.4$. Though the situation for type-III and -IV are quite similar to that of type-II 2HDM. As we are working under the assumption of a CP-even vacuum of the 2HDM potential, vertices like AWW and AZZ are not present at the tree-level. Among the tree-level scalar-gauge couplings which are important for the cascade decays of the new scalars, AZh and $H^\pm h W^\mp$ are proportional to $\cos(\beta - \alpha)$, whereas AZH and $H^\pm H W^\mp$ are proportional to $\sin(\beta - \alpha)$. It is possible to realise an exact alignment in the multi-Higgs-doublet models in the framework of certain additional symmetries of the 2HDM potential [33–37].

It is evident from eqs. (2.7) when $\tan \beta \gtrsim 1$, the hbb coupling multiplier deviates significantly from unity in type-II 2HDM. For such values of $\tan \beta$ the branching ratio $\text{Br}(h \rightarrow b\bar{b})$ as well as the production of h in both gg and $b\bar{b}$ -fusion substantially increase. It is mainly due to the measurement of the processes like $gg \rightarrow \gamma\gamma, b\bar{b}, VV^*$ and $Vh \rightarrow b\bar{b}$, that the parameter space of a type-II 2HDM in the $\cos(\beta - \alpha) - \tan \beta$ plane is quite strongly constrained. The impact of the measurement of the Higgs signal strengths in each individual search channels on the $\cos(\beta - \alpha) - \tan \beta$ plane has been discussed in ref. [38]. It should be mentioned that the coupling multipliers of the SM-like Higgs also becomes close to unity when $\sin(\beta + \alpha) = 1$ *i.e.*, at the so-called ‘wrong-sign Yukawa’ limit [39] for type-II, -III, and -IV 2HDM. Though, with better measurement of the processes like $Vh \rightarrow b\bar{b}$, $h \rightarrow \Upsilon\gamma$ [40, 41] the fate of the wrong-sign Yukawa region will be decided in near future.

It is also clear from eq. (2.7) that, though the coupling multipliers of the SM-like Higgs become unity at the alignment limit, the couplings of the exotic Higgses with SM fermions can be non-zero. The HVV coupling becomes identically zero at the alignment limit, protecting the alignment limit against measurements like $gg \rightarrow H \rightarrow WW, ZZ$. Though the couplings of H and A with SM fermions do not vanish at $\cos(\beta - \alpha) = 0$. Thus it is possible to constrain the parameter space of the type-II 2HDM even at the alignment limit from the non-observation of the heavier scalars [19] in processes like $gg/b\bar{b} \rightarrow H/A \rightarrow \tau\bar{\tau}, \gamma\gamma$, $gg \rightarrow$

$H \rightarrow hh$, etc. Both ATLAS and CMS are involved in numerous dedicated searches of these kinds, resulting in significant constraints on the 2HDM parameter space.

Different kinds of mass spectra of the new scalars in a 2HDM can lead to quite rich phenomenology at the LHC. In addition to the regular search channels consisting of a pair of SM particles as mentioned earlier, exotic states decaying into one another can also provide strong constraints on 2HDM parameter space. At this point we define $m_A = m_H = m_{H^\pm}$ as the ‘degenerate’ case and the case when any of the three exotic scalars is more massive than the rest two, as the ‘hierarchical’ case. The constraints from the decay of the new scalars into SM particles are significantly relaxed in the hierarchical scenario compared to the degenerate case [42]. But for the hierarchical spectrum of new scalars, the channels like $H(A) \rightarrow ZA(H)$ dominate the total decay width of such states, leading to new bounds on the parameter space which are not applicable for the degenerate case. A hierarchical spectrum such as $m_A > m_H \sim m_{H^\pm} \sim v$ can lead to a first-order electroweak phase transition providing an explanation for the matter-antimatter asymmetry, with $A \rightarrow ZH$ being its smoking gun signature at LHC [43, 44]. In general, the importance of Higgs cascade decays as the possible probes of an extended scalar sector have been discussed in the literature [45–50] and $A \rightarrow ZH$ decay is dubbed as a ‘golden channel’ in this context [51].

III. CONSTRAINTS ON 2HDM PARAMETER SPACE

We work with the 2HDM parameters in the physical basis which consists of $\{m_h, m_H, m_A, m_{H^\pm}, \tan\beta, \cos(\beta - \alpha), m_{12}^2, \lambda_6, \lambda_7, v\}$. Along with $m_h = 125.09$ GeV, $v = 246$ GeV and $\lambda_{6,7} = 0$ we are left with six free parameters. The theoretical constraints are discussed below.

- *Vacuum stability* The stability of the EW vacuum in a 2HDM at the tree-level is ensured if [12],

$$\lambda_1 > 0, \quad \lambda_2 > 0, \quad \lambda_3 > -\sqrt{\lambda_1 \lambda_2}, \quad \lambda_3 + \lambda_4 - |\lambda_5| > -\sqrt{\lambda_1 \lambda_2}. \quad (3.1)$$

It can be shown that at the alignment limit, the first two conditions are satisfied if $m_{12}^2 = m_H^2 s_\beta c_\beta$. Along with that, the last two criteria are satisfied if $m_h^2 + m_{H^\pm}^2 - m_H^2 > 0$ and $m_h^2 + m_A^2 - m_H^2 > 0$ respectively. This means for degenerate masses of the new scalars the

last two criteria are automatically satisfied if the first two are satisfied. For hierarchical mass spectrum, the mass of the exotic scalars cannot be arbitrarily different.

- *Perturbativity* The perturbativity of the quartic couplings is satisfied if $\lambda_i \lesssim 4\pi$. At the alignment limit this implies for $t_\beta \gtrsim 1$, $|m_{12}^2 - m_H^2 s_\beta c_\beta| \lesssim v^2$.
- *Unitarity* Tree-level unitarity of the S-matrix requires the eigenvalues of the $2 \rightarrow 2$ scattering matrix to be less than 8π . At the alignment limit for $m_{12}^2 \sim m_H^2 s_\beta c_\beta$, this implies that the differences between the masses of the new scalars have to be $\lesssim v$.
- *Oblique parameters* The new scalars in 2HDM contributes to the oblique parameters through their couplings to the massive gauge bosons [52–54]. At the alignment limit such contributions to the T -parameter assume the form,

$$\Delta T = \frac{g^2}{64\pi^2 m_W^2} \left(F(m_{H^\pm}^2, m_A^2) + F(m_{H^\pm}^2, m_H^2) - F(m_A^2, m_H^2) \right), \quad (3.2)$$

with,

$$\begin{aligned} F(a, b) &= \frac{a+b}{2} - \frac{ab}{a-b} \ln \left(\frac{a}{b} \right) & (a \neq b) \\ &= a & (a = b). \end{aligned}$$

As eq. (3.2) suggests, this anomalous contribution to the T -parameter vanishes at the limit $m_{H^\pm} = m_A$ or $m_{H^\pm} = m_H$. However, substantially away from the alignment limit this does not hold for the entire range of m_A . As mentioned earlier, the measurements of the Higgs signal strengths imply that the maximum values of $\cos(\beta - \alpha)$ can be attained in type-I 2HDM, $|\cos(\beta - \alpha)| \lesssim 0.4$. For the rest three types of Yukawa structure, $|\cos(\beta - \alpha)| \lesssim 0.1$. We have checked that the limits $m_H = m_{H^\pm}$ and $m_A = m_{H^\pm}$ ensure that the contribution to the T -parameter remains in the experimentally allowed range at 95% CL even when we consider small deviations from alignment limit, $\cos(\beta - \alpha) \lesssim 0.1$. For $\cos(\beta - \alpha) \sim 0.4$, even for $m_H = m_{H^\pm} = 300$ GeV, $m_A \gtrsim 480$ GeV is ruled out from the measurement of T -parameter.

LEP searches put constraint on the mass of the charged scalar as $m_{H^\pm} \gtrsim 72$ GeV (80 GeV) for type-I (II) 2HDM [55]. Also the searches for $Z \rightarrow AH \rightarrow \tau\bar{\tau}\tau\bar{\tau}$ lead to the constraint $m_H + m_A \gtrsim 208$ GeV [56]. The charged scalar mediates flavour-violating processes such as $B_d \rightarrow X_s \gamma$, $B_s \rightarrow \mu^+ \mu^-$, $B_d^+ \rightarrow \tau^+ \nu$, etc. The measurement of the width of $B_d \rightarrow X_s \gamma$ leads to the most stringent constraint on the charged scalar mass for type-II 2HDM, $m_{H^\pm} \gtrsim$

480 GeV [57, 58]. For type-I 2HDM, the constraint from meson decays is comparatively less stringent, $m_{H^+} \gtrsim 160$ GeV [57]. Based on the similarity in couplings of the scalars to the quarks, the constraints on charged scalar mass for type-I and -II 2HDM can also be used for type-IV and -III cases respectively. Though we do not consider this as a hard bound for our purpose as it can be ameliorated in several extensions of 2HDM [59]. Moreover, the mass differences of the three exotic scalars are constrained from the measurement of the oblique parameters. For $\cos(\beta - \alpha) = 0$, the contributions of the new scalars to the S and T parameters do not depend upon m_{12}^2 or $\tan\beta$. For a fixed value of m_H , the constraints from precision tests are satisfied only if $m_H \sim m_A$ or $m_H \sim m_{H^\pm}$. As mentioned earlier, the measurements of the signal strengths of the SM-like Higgs boson constrain the value of $\cos(\beta - \alpha)$ to be close to zero, especially for type-II, -III and -IV 2HDM. Thus, while working with the hierarchical spectrum of the new scalars, we take $\cos(\beta - \alpha)$ to be close to zero. But for the degenerate spectrum of exotic scalars, we consider possible large deviation from the alignment limit while we present the excluded region on the $\cos(\beta - \alpha) - \tan\beta$ plane. In this paper, we have considered the constraints due to the non-observation of the processes: $gg \rightarrow H \rightarrow ZZ$ [60], $gg \rightarrow H \rightarrow hh$ [61], $gg \rightarrow H(A) \rightarrow A(H/h)Z$ [62] and $gg/b\bar{b} \rightarrow H/A \rightarrow \tau\bar{\tau}$ [63].

IV. COUPLINGS OF THE HEAVIER SCALARS IN 2HDMEFT

We contain our discussion only to the bosonic operators of 2HDMEFT for simplicity. Phenomenology of the fermionic dim-6 terms will be reported elsewhere. As discussed in ref. [28], the measurement of EW oblique parameters, triple gauge boson vertices and Higgs signal strengths, constrain the bosonic operators other than type $\varphi^4 D^2$ at $\mathcal{O}(10^{-3})$. Moreover, some of the $\varphi^4 D^2$ -type of operators violate the T -parameter at the tree-level and the corresponding Wilson coefficients are rather small. Thus we have considered only the operator of type $\varphi^4 D^2$ which do not contribute to the T -parameter in the tree-level:

$$\begin{aligned} O_{H1} &= (\partial_\mu |\varphi_1|^2)^2, \quad O_{H2} = (\partial_\mu |\varphi_2|^2)^2, \quad O_{H12} = (\partial_\mu (\varphi_1^\dagger \varphi_2 + h.c.))^2, \\ O_{H1H2} &= \partial_\mu |\varphi_1|^2 \partial^\mu |\varphi_2|^2, \quad O_{H1H12} = \partial_\mu |\varphi_1|^2 \partial^\mu (\varphi_1^\dagger \varphi_2 + h.c.), \quad O_{H2H12} = \partial_\mu |\varphi_2|^2 \partial^\mu (\varphi_1^\dagger \varphi_2 + h.c.). \end{aligned} \quad (4.1)$$

In presence of such operators, the non-diagonal kinetic terms arise after SSB [22]. In order to get rid of such terms, one needs to rescale the neutral CP-even d.o.f. *i.e.*, ρ_1 and ρ_2 . This

implies that the physical neutral CP-even scalars in presence of these operators are rescaled compared to the tree-level 2HDM.

$$\begin{aligned} h &\rightarrow (1 - x_1)h + yH, \\ H &\rightarrow (1 - x_2)H + yh. \end{aligned} \tag{4.2}$$

x_1 , x_2 and y can be written in terms of the Wilson coefficients of the operators appearing in eq. (4.1) and the scale of new physics beyond 2HDM. The analytical forms of x_1 , x_2 and y can be found in Appendix A. Eq. (4.2) dictates that any coupling involving at least one h or H field are modified compared to 2HDM at the tree-level. For example,

$$\kappa'_{hff} = (1 - x_1)\kappa_{hff} + y\kappa_{Hff}, \tag{4.3}$$

$$\kappa'_{Hff} = (1 - x_2)\kappa_{Hff} + y\kappa_{hff}, \tag{4.4}$$

$$\kappa'_{hVV} = (1 - x_1)\sin(\beta - \alpha) + y\cos(\beta - \alpha), \tag{4.5}$$

$$\kappa'_{HVV} = (1 - x_2)\cos(\beta - \alpha) + y\sin(\beta - \alpha), \tag{4.6}$$

$$\kappa'_{AZh} = (1 - x_1)\kappa_{AZh} + y\kappa_{AZH}, \tag{4.7}$$

$$\kappa'_{AZH} = (1 - x_2)\kappa_{AZH} + y\kappa_{AZh}. \tag{4.8}$$

Eqs. (4.4) and (4.6) affect decay processes like $H \rightarrow \tau\bar{\tau}$ and $H \rightarrow ZZ$ which are particularly important in the degenerate case. Similarly the decay widths $H(A) \rightarrow ZA(H)$, which become relevant in the hierarchical scenarios are changed according to eq. (4.8). What is more interesting that processes, which apparently look unaffected by the rescaling of fields, such as $gg \rightarrow A \rightarrow \tau\bar{\tau}$, are also changed. It is due to the fact that away from the alignment limit, for a large range of values of m_A and $\tan\beta$, $\text{Br}(A \rightarrow Zh)$ is quite significant. The change in $\text{Br}(A \rightarrow Zh)$ according to eq (4.7) in turn modifies $\text{Br}(A \rightarrow \tau\bar{\tau})$. Even the change in $h \rightarrow f\bar{f}$ can be important for bounds on the heavier scalars. For example, the search for $A \rightarrow Zh$ assumes that the Higgs in the final state further decays into a pair of b -tagged jets [62].

Many of the sum rules involving various gauge couplings, which hold in 2HDM at the tree-level, are no longer valid in the presence of 6-dim operators [4]. These sum rules can play an important role in deciphering new physics beyond 2HDM. For instance, in 2HDM at the tree-level, the sum rule $\kappa_{hVV}^2 + \kappa_{HVV}^2 = 1$ holds true, but in presence of the dim-6 terms mentioned in eq. (4.1), $\kappa_{hVV}^2 + \kappa_{HVV}^2 = 1 - 2(x_1 s_{\beta-\alpha}^2 + x_2 c_{\beta-\alpha}^2 + 2y c_{\beta-\alpha} s_{\beta-\alpha})$. If another CP-even neutral

scalar, H is discovered after $h(125)$, the measurement of its decay width and $\text{Br}(H \rightarrow WW)$ will facilitate the verification of such a sum rule. A deviation from $\kappa_{hVV}^2 + \kappa_{HVV}^2 = 1$ will point to a departure from the CP-conserving 2HDM. If $\kappa_{hVV}^2 + \kappa_{HVV}^2 < 1$, then it may indicate towards CP-violating 2HDM or CP-conserving NHDM ($N > 2$). Even the dim-6 operators in 2HDMEFT can lead to $\kappa_{hVV}^2 + \kappa_{HVV}^2 < 1$. On contrary, neither CP-violating 2HDM nor NHDM can lead to $\kappa_{hVV}^2 + \kappa_{HVV}^2 > 1$. Though, such a scenario can be interpreted in terms of the dim-6 terms of 2HDMEFT. At the CP-conserving limit with $\lambda_{6,7} \neq 0$ the similar argument for tree-level 2HDM is valid in this context, whereas in general $\lambda_{6,7} \neq 0$ will follow the argument for CP-violating 2HDM.

V. BENCHMARK SCENARIOS

Following the discussions in Section III in the context of oblique parameters, for the hierarchical mass spectrum, we consider either $m_A = m_{H^\pm}$ or $m_H = m_{H^\pm}$. The limit $m_A = m_H$ is highly constrained from the measurement of S, T parameters and the decays of H and A into each other are kinematically forbidden.

So the mass spectra under scrutiny for the hierarchical case are [49]:

$$\begin{aligned} \mathbf{C1} : m_A = m_{H^\pm} > m_H & \quad \mathbf{C2} : m_A > m_H = m_{H^\pm} \\ \mathbf{C3} : m_A = m_{H^\pm} < m_H & \quad \mathbf{C4} : m_A < m_H = m_{H^\pm}. \end{aligned} \quad (5.1)$$

For the hierarchical case, we have studied the bounds on the $m_A = m_H$ plane for $\tan \beta = 1.5$ and $\cos(\beta - \alpha) = 0$ with and without considering the dim-6 terms.

On the other hand, for the degenerate mass spectrum ($m_H = m_A = m_{H^\pm}$) new scalars can no longer decay into each other, thus making the SM decay channels of these scalars $H \rightarrow ZZ, \tau\bar{\tau}, b\bar{b}$, $A \rightarrow Zh, \tau\bar{\tau}$ more important. We have studied the change in the constraints due to inclusion of dim-6 operators on the $\cos(\beta - \alpha) - m_A$ plane. We define the benchmark for the degenerate case as,

$$\mathbf{C5} : m_H = m_A = m_{H^\pm}, \tan \beta = 1.5. \quad (5.2)$$

As mentioned earlier, $\lambda_{6,7} = 0$ for both degenerate and hierarchical cases. Also the quadratic mass parameter is taken to be $m_{12}^2 = m_H^2 s_\beta c_\beta$ following the discussions on the theoretical constraints in Section III. For both the hierarchical and degenerate cases, the bounds on

2HDM at the tree-level are compared with a specific case of 2HDMEFT with the following values of the Wilson coefficients and the new physics scale [28],

$$\mathbf{BP1}: c_{H1} = -1, c_{H2} = 1.5, c_{H12} = c_{H1H2} = c_{H1H12} = c_{H2H12} = 0, f = 1 \text{ TeV.} \quad (5.3)$$

The branching ratios of various scalars in 2HDM at the tree-level, as well as in the presence of the 6-dim operators, have been calculated with 2HDMC [64] after incorporating the modified couplings. The production cross-section of the neutral scalars have been computed up to NNLO in QCD using **SusHi** [65]. The constraints on the $m_A - m_H$ plane from various exotic Higgs search channels are elucidated in figs. 1, 2, 3 and 4 corresponding to the mass spectra **C1**, **C2**, **C3** and **C4** respectively. In fig. 1, the appreciable change from the tree-level 2HDM scenario takes place only for type-I and type-IV Yukawa couplings. Moreover, it can be seen that the characteristics of the type-I and -IV 2HDM are similar in this context, as is the case for type-II and type-III. This pattern can be attributed to the similarity in the couplings of the new scalars with the SM quarks, following eq. (2.7), which dictate their production cross-sections at LHC. The most significant search channel in context of the mass spectra **C1** is $A \rightarrow ZH(b\bar{b})$. For all four Yukawa types, the change in $\text{Br}(H \rightarrow b\bar{b})$ can be substantially different in 2HDMEFT compared to tree-level 2HDM, though $\text{Br}(A \rightarrow ZH)$ does not change significantly. This happens because a key decay channel of H , *i.e.*, $H \rightarrow WW$, becomes viable in **BP1** of 2HDMEFT, which is absent in tree-level 2HDM at $\cos(\beta - \alpha) = 0$. For example, with $m_A = 400 \text{ GeV}$ and $m_H = 300 \text{ GeV}$, $\text{Br}(H \rightarrow b\bar{b})$ becomes ~ 0.45 in **BP1** of 2HDMEFT compared to its value ~ 0.73 in tree-level 2HDM. Such a reduction in $\text{Br}(H \rightarrow b\bar{b})$ is compensated by the newly viable channel $H \rightarrow WW$. This leads to a reduced value of $A \rightarrow ZH(b\bar{b})$, and eventually, to a more relaxed constraint on m_H . Compared to type-I and -IV 2HDM, $\text{Br}(H \rightarrow b\bar{b})$ is larger for type-II and -III Yukawas even in the tree-level scenario. Thus the percentage change in $\text{Br}(H \rightarrow b\bar{b})$ is much lower for type-II and -III compared to type-I and -IV. So the change in the excluded region from the non-observation of $A \rightarrow ZH$ is larger in type-I and -IV compared to type-II and -III. $A \rightarrow \tau\bar{\tau}$ rules out a region of parameter space where the on-shell decay $A \rightarrow ZH$ is not allowed. As eq. (2.7) suggests, $\text{Br}(A \rightarrow \tau\bar{\tau})$ attains the smallest value for type-III case among all the Yukawa types. In both type-I and -III the $A\tau\bar{\tau}$ coupling is proportional to $\cot\beta$ as opposed to $\tan\beta$ in type-II and -IV. $\text{Br}(A \rightarrow \tau\bar{\tau})$ is even smaller in type-III 2HDM compared to type-I 2HDM because $\text{Br}(A \rightarrow b\bar{b})$ becomes larger in the latter case. On inclusion of the 6-dim operators,

the region excluded from $gg \rightarrow A \rightarrow \tau\bar{\tau}$ is not significantly altered for type-I, -II and -IV cases.

In the context of Yukawa types, a similar pattern in the excluded region can be seen for mass spectra **C2** as depicted in fig. 2. It can also be seen that the excluded region from $A \rightarrow ZH$ is small in the case **C2** compared to **C1**. For mass spectrum **C2**, the decay channel $A \rightarrow W^\pm H^\mp$ becomes kinematically viable and has branching ratio almost similar to that of $A \rightarrow ZH$. However the branching ratios of H are the same in the cases **C1** and **C2**. This, along with $\text{Br}(A \rightarrow ZH)|_{\mathbf{C1}} \gtrsim 2 \times \text{Br}(A \rightarrow ZH)|_{\mathbf{C2}}$ dictate that the excluded region for **C1** is larger than that in **C2**. As the branching ratios of H in cases **C1** and **C2** are the same in both 2HDM and 2HDMEFT, the pattern of deviation in terms of different Yukawa couplings are similar for **C1** and **C2**. The changes in the branching ratios of have been illustrated in fig. 8 in Appendix B.

$H \rightarrow ZA(b\bar{b})$ can rule out a significant area of parameter space on the $m_A - m_H$ plane for cases **C3** and **C4**. The excluded region in the case **C4** does not show a substantial change upon the inclusion of dim-6 terms as in **C1** or **C2**. This happens because $\text{Br}(A \rightarrow b\bar{b})$ remains almost the same in 2HDM and 2HDMEFT. It changes only by $\lesssim 10\%$ due to a small non-zero value of $\text{Br}(A \rightarrow Zh)$ in **BP1** of 2HDMEFT. As opposed to 2HDMEFT, for $\cos(\beta - \alpha) = 0$, $A \rightarrow Zh$ is absent in 2HDM at the tree-level. So the constraints on m_A from $H \rightarrow ZA$ can be relaxed at most by ~ 19 GeV for type-I and -IV for **C4** around $m_H \sim 795$ GeV, a region which is already disfavoured from the criteria of stability and unitarity. It can be seen that a significant area is ruled out from $H \rightarrow WW$ for $m_H \lesssim 350$ GeV and $m_H - m_A \lesssim 90$ GeV if the 6-dim operators are included. $H \rightarrow WW$ is otherwise absent in the alignment limit irrespective of the mass spectrum of the new scalars. $H \rightarrow t\bar{t}$ becomes dominant if $m_H \gtrsim 2m_t \sim 350$ GeV. For $m_H \lesssim 350$ GeV, $\text{Br}(H \rightarrow ZA)$ becomes substantial if $m_H - m_A \gtrsim 90$ GeV. Thus the area disfavoured by $H \rightarrow WW$ is confined to a small strip close to the $m_H \sim m_A$ line as shown in fig. 4. A similar effect can be seen in fig. 3 for the case **C3**. The appearance of such an exclusion region originates from the fact that in presence of the 6-dim terms, the coupling multiplier κ_{HVV} does not vanish at $\cos(\beta - \alpha) = 0$ as opposed to the tree-level 2HDM. The region ruled out from $H \rightarrow \tau\bar{\tau}$ overlap with that for $H \rightarrow WW$ in 2HDMEFT in most of the cases. However, for type-I and -III 2HDM, the constraint from $H \rightarrow \tau\bar{\tau}$ appears to be relaxed compared to the two other

types. It can also be seen that the region excluded from $H \rightarrow ZA$ is smaller for **C3** compared to **C4** even in 2HDM at tree-level. This occurs because the decay channel $H \rightarrow W^\pm H^\mp$ becomes kinematically viable for **C3** and $\text{Br}(H \rightarrow W^\pm H^\mp) \sim \text{Br}(H \rightarrow ZA)$. This leads to a smaller cross-section in the channel $gg \rightarrow H \rightarrow ZA$, hence a relaxed constraint on m_A for **C3** compared to the case **C4** even in tree-level 2HDM.

Till now we have discussed the changes in the excluded region on the $m_A - m_H$ plane at a low value of $\tan \beta$. At large $\tan \beta$, *i.e.*, $\tan \beta \gtrsim 10$, exotic decays such as $H \rightarrow ZA$, $A \rightarrow ZH$ become negligible even in the hierarchical scenarios and $gg/b\bar{b} \rightarrow H/A \rightarrow \tau\bar{\tau}$ leads to the only relevant constraint. This can be read off eq. (2.7). In such cases, for $\cos(\beta - \alpha) = 0$, the constraints on m_H or m_A are altered at the most by ~ 5 GeV.

In fig. 5 (a) we have depicted the constraints on the $\cos(\beta - \alpha) - m_A$ plane due to the non-observation of H and A in the degenerate mass scenario for type-II 2HDM. As mentioned earlier, the exotic decay channels like $H(A) \rightarrow A(H)Z$, etc. are absent in such a case. It can be seen from the eq. (2.7) that couplings like HVV , AZh , etc., vanish at the exact alignment limit in 2HDM at the tree-level [19]. Thus the non-observation of $H \rightarrow ZZ$ or $A \rightarrow Zh$ cannot rule out $\cos(\beta - \alpha) = 0$ irrespective of the value of m_A . This also implies that the discovery of a new scalar in the VV or Zh final states would rule out the exact alignment limit in the framework of a CP-conserving 2HDM. Though it is not the case if the 6-dim terms are also present, as those can lead to non-vanishing contribution to such decay channels. It can be seen from fig. 5 (a), in a 2HDM augmented with $\varphi^4 D^2$ kind of operators, the bounds from $H \rightarrow ZZ$, $A \rightarrow \tau\bar{\tau}$, Zh modify in comparison to 2HDM at the tree level. $H \rightarrow ZZ$ can become non-vanishing, ruling out a range of values of m_H even at $\cos(\beta - \alpha) = 0$. There is an overall leftward shift in the region ruled out by $A \rightarrow \tau\bar{\tau}$ which can be followed from eqs. (2.7) and (4.2). For example, the values $m_H \sim 210 - 355$ GeV and $m_A \sim 300 - 340$ GeV can be excluded from $H \rightarrow ZZ$ and $A \rightarrow Zh$ respectively at 95% CL even in the alignment limit. In fig. 5 (b) we have shown the cross-section of H and A *via* the gluon-fusion times the branching ratios in the channels ZZ and Zh at the alignment limit in presence of the higher dimensional operators. The value of $\sigma \times \text{Br}$ for $H \rightarrow ZZ$ reaches ~ 0.30 pb in the range $m_H = 200 - 344$ GeV. For $A \rightarrow Zh$ it can reach up to 1.5 pb in the range $m_A \sim 280 - 330$ GeV. For 2HDM at the tree-level, such processes would not at all exist in the alignment limit.

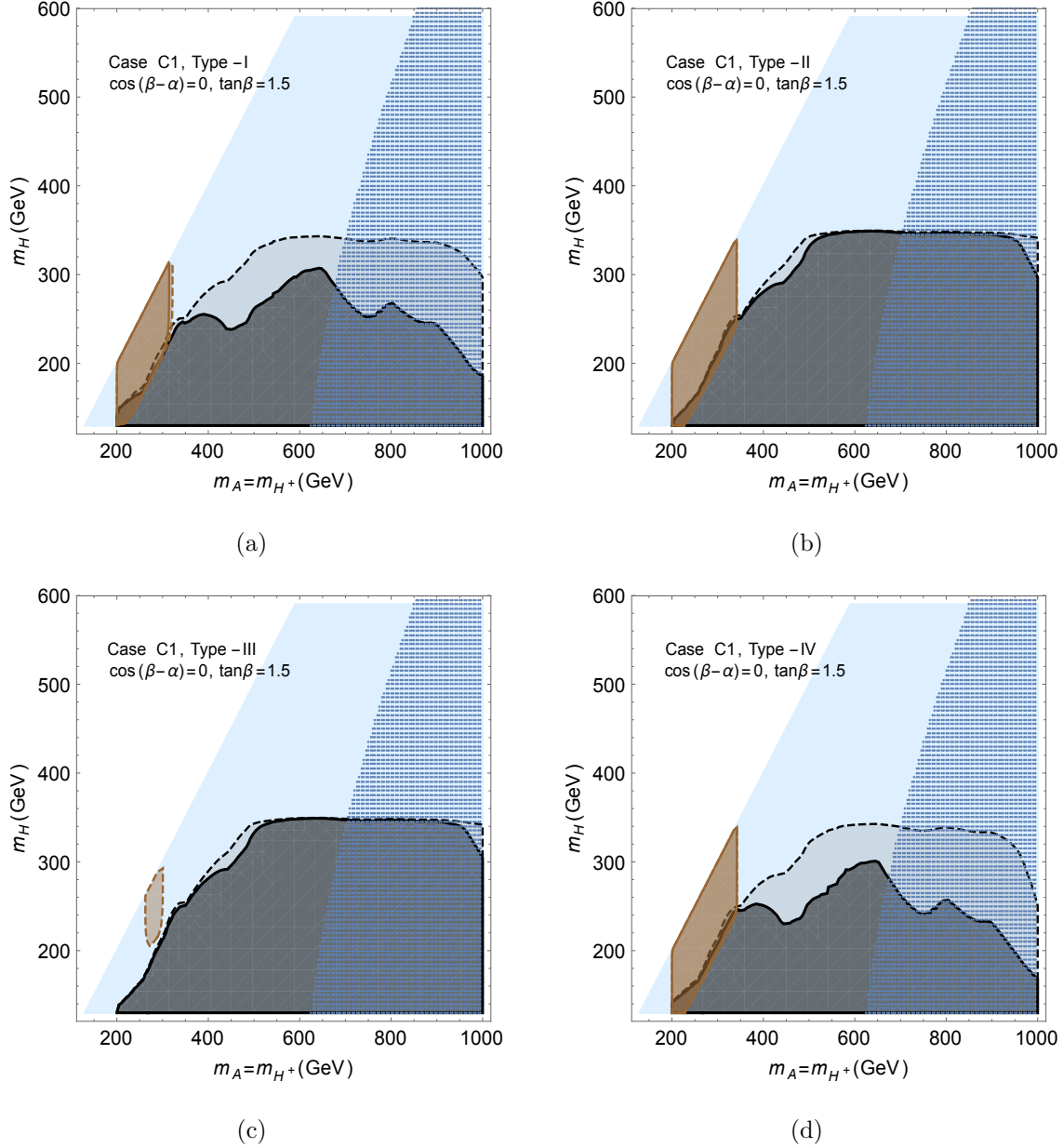


FIG. 1. The effect of $\varphi^4 D^2$ type of operators for mass spectrum **C1**. Only the light blue region is kinematically viable. The grey regions with the dashed and solid boundaries are ruled out from $gg \rightarrow A \rightarrow ZH(b\bar{b})$ in 2HDM and **BP1** of 2HDMEFT respectively. The brown regions with the dashed and solid boundaries are ruled out from $gg \rightarrow A \rightarrow \tau\bar{\tau}$ in 2HDM and **BP1** of 2HDMEFT. The dotted blue region is disfavoured from the theoretical constraints, *viz.* stability, perturbativity and unitarity.

It is to be noted that, according to eq. (2.7), for a particular value of $|\cos(\beta - \alpha)|$

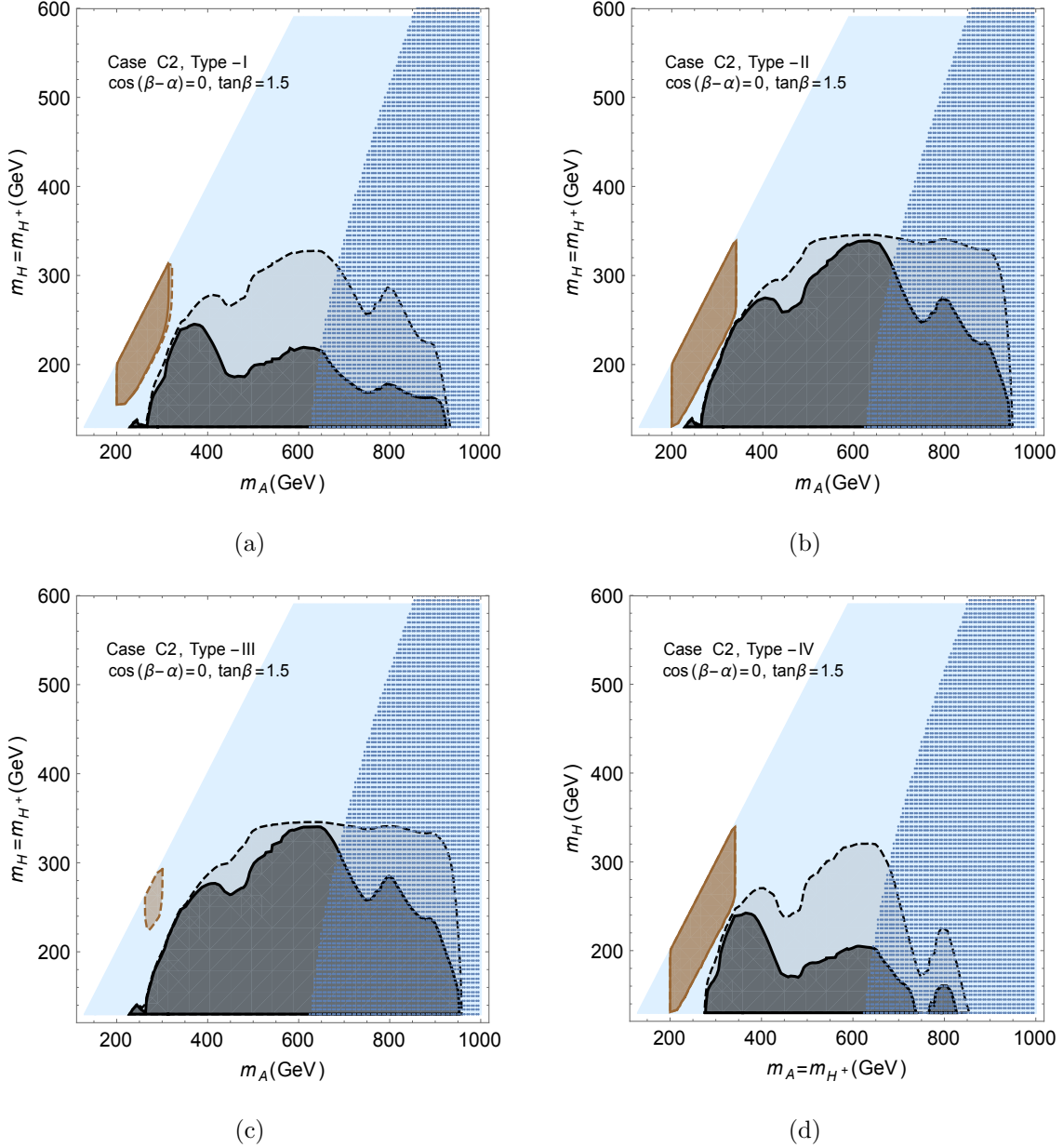


FIG. 2. The effect of $\varphi^4 D^2$ type of operators for mass spectrum **C2**. Colour coding is the same as in fig. 1.

and $\tan\beta \gtrsim 1$, the $hb\bar{b}$ coupling multiplier is more pronounced in the negative direction of $\cos(\beta - \alpha)$, compared to the positive direction. This effect also propagates in the gluon-fusion cross-section of H . Thus the area on the $\cos(\beta - \alpha) - m_A$ plane ruled out by $gg \rightarrow H \rightarrow ZZ$ is larger on the negative $\cos(\beta - \alpha)$ direction. The relevant branching ratios of the heavy scalars have been shown in fig. 9.

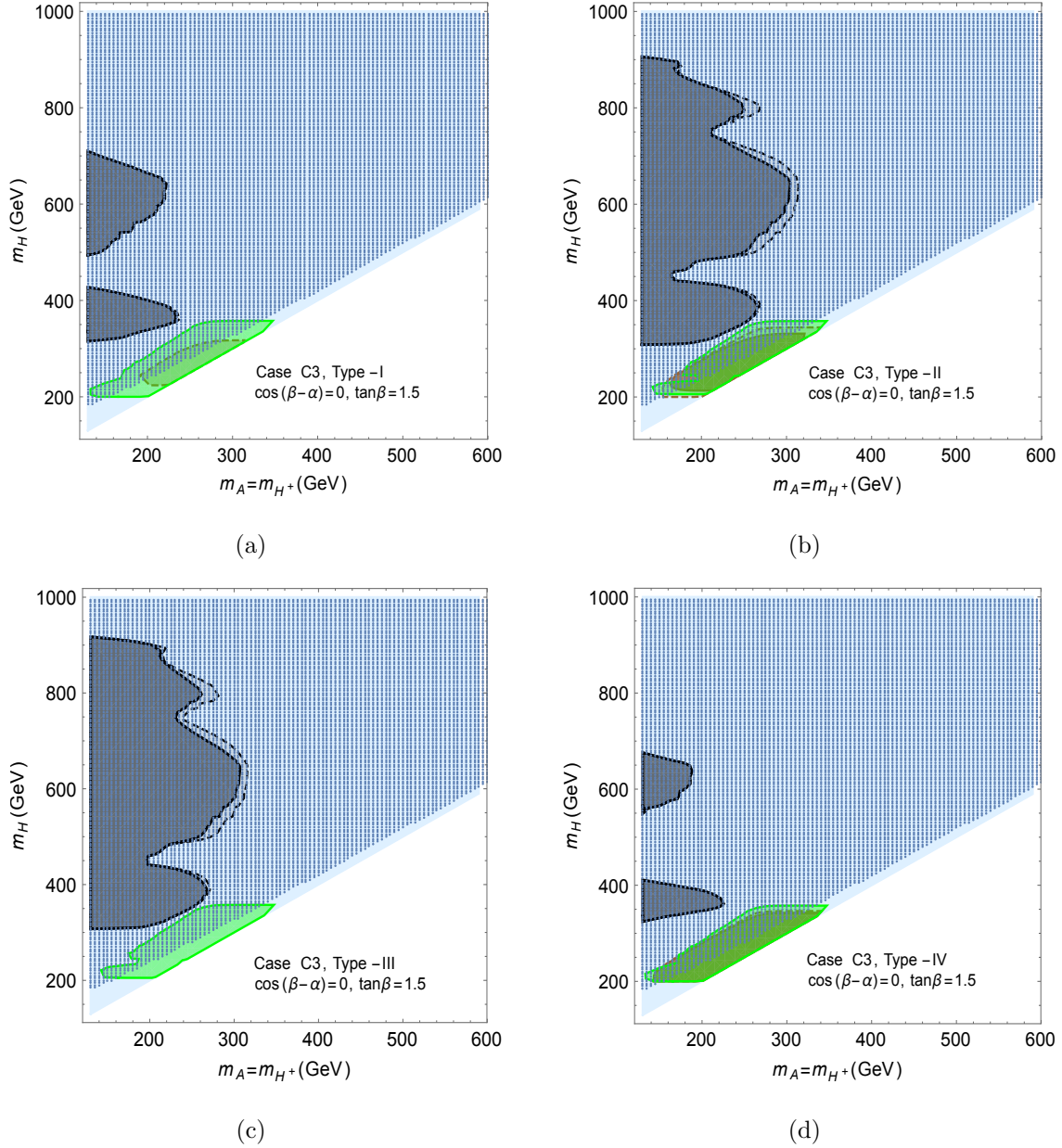


FIG. 3. The effect of $\varphi^4 D^2$ type of operators for mass spectrum **C3**. The grey regions with the dashed and solid boundaries are ruled out from $gg \rightarrow H \rightarrow ZA(b\bar{b})$ in 2HDM and **BP1** of 2HDMEFT respectively. The brown regions with the dashed and solid boundaries are ruled out from $gg \rightarrow H \rightarrow \tau\bar{\tau}$ in 2HDM and **BP1** of 2HDMEFT. The green region is disfavoured from the non-observation of $gg \rightarrow H \rightarrow ZZ$ in **BP1** of 2HDMEFT, which is absent in 2HDM at the tree-level for $\cos(\beta - \alpha) = 0$. Rest of the colour coding is the same as in fig. 1.

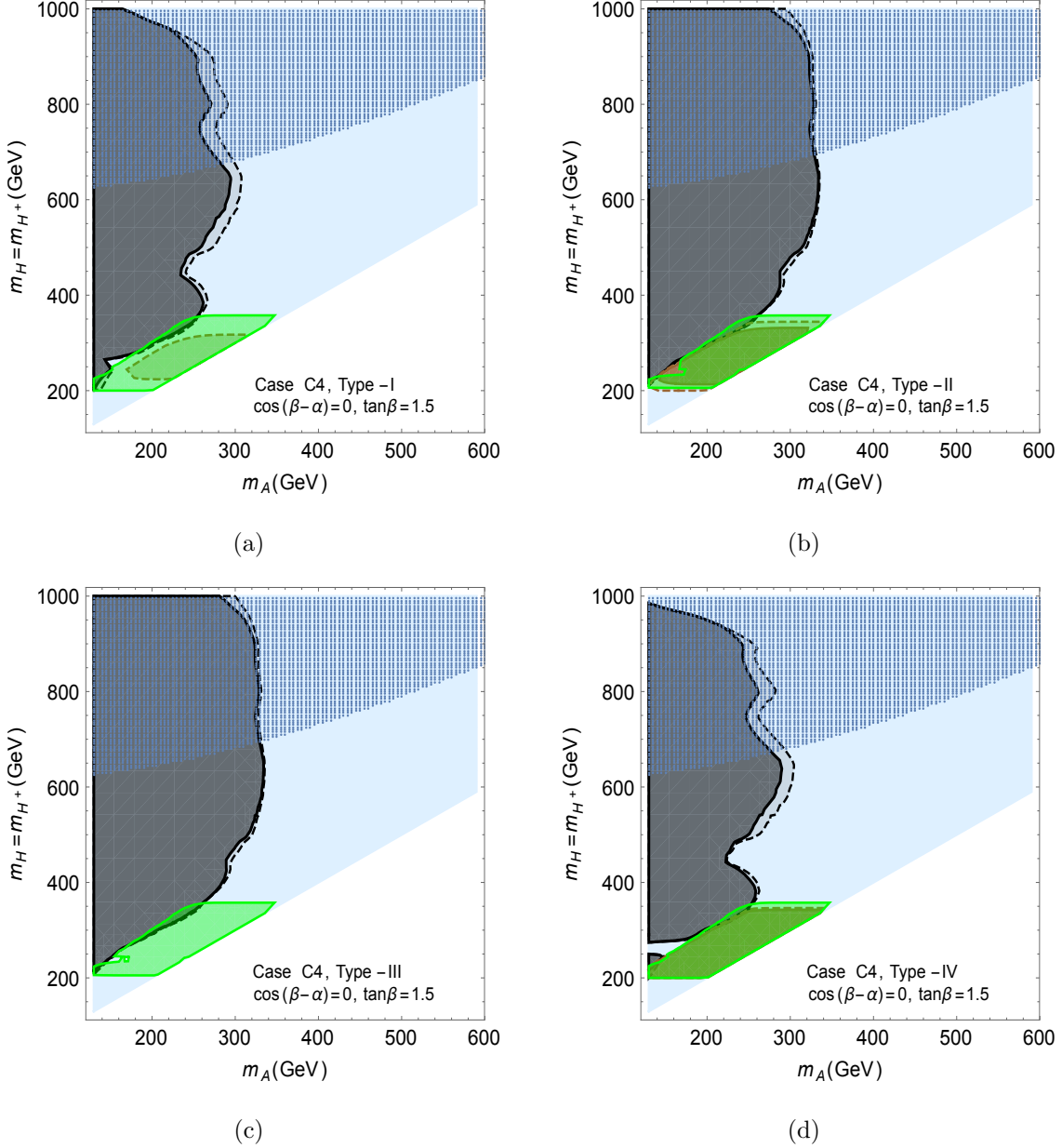


FIG. 4. The effect of $\varphi^4 D^2$ type of operators for mass spectrum **C4**. Colour coding is the same as in fig. 3.

In fig. 6 we have shown the change in the excluded region from various searches of the new scalars on the $m_H - \tan\beta$ plane. Here, $\cos(\beta - \alpha) = 0.1$ and $m_A = m_{H^\pm} = m_H + 100$ GeV. So, this is essentially a hierarchical mass scenario where the exotic decay channel $A \rightarrow ZH$ plays a significant role at lower values of $\tan\beta$. For type-II 2HDM both $hb\bar{b}$ and $h\tau\bar{\tau}$ couplings grow with increasing $\tan\beta$. Thus in fig. 6 higher values of $\tan\beta$ are mostly ruled out from

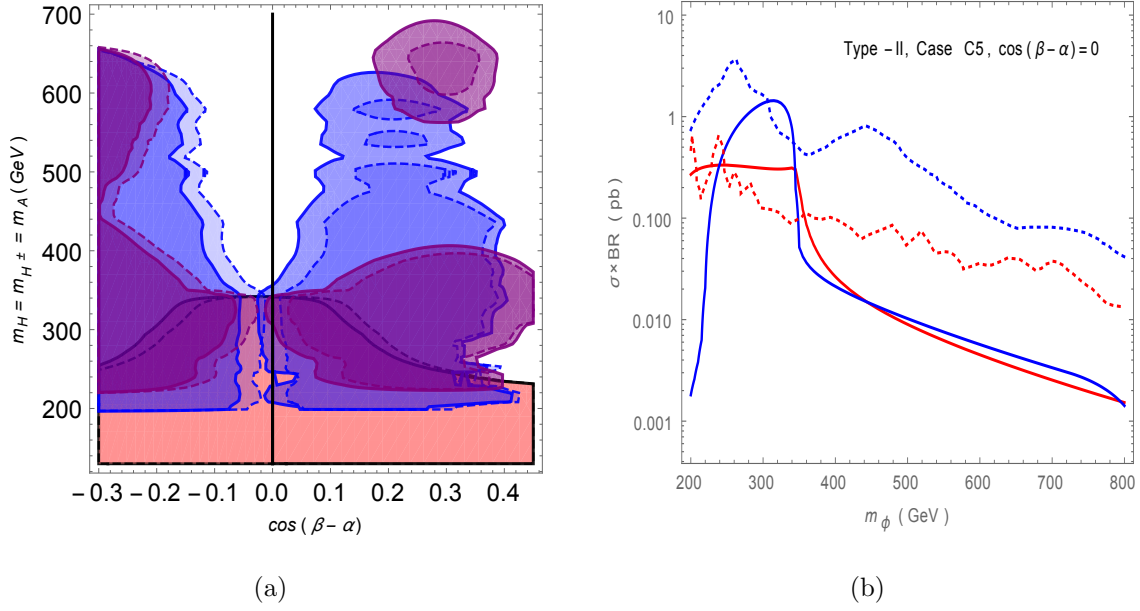


FIG. 5. The effect of $\varphi^4 D^2$ type of operators for **C5** in Type-II 2HDM. (a) The blue regions with the dashed and solid boundaries are ruled out from $H \rightarrow ZZ$, the pink regions with the dashed and solid boundaries are ruled out from $A \rightarrow \tau\tau$ and the purple regions with the dashed and solid boundaries are ruled out from $A \rightarrow Zh$ in 2HDM and **BP1** of 2HDMEFT respectively. (b) The solid blue (red) line represents $\sigma \times \text{Br}$ for $gg \rightarrow H \rightarrow ZZ$ ($gg \rightarrow A \rightarrow Zh$) at the alignment limit in presence of the 6-dim operators mentioned in **BP1**. The experimental upper limit to the $\sigma \times \text{Br}$ corresponding to the two processes are also shown as dotted lines in the same colour.

the measurements of $b\bar{b} \rightarrow H \rightarrow \tau\bar{\tau}$. On introduction of the 6-dim terms the region excluded from $H \rightarrow WW$ increases, whereas that from $A \rightarrow ZH$ shrinks. For instance, in 2HDMEFT the values $m_H \approx 464 - 686$ GeV can be ruled out for $\tan \beta \lesssim 1.5$. Moreover, the excluded region becomes larger in the direction of $\tan \beta$ for $m_H \approx 254 - 464$ GeV.

So far we have considered the phenomenology of only the neutral scalars. Now we comment on a few effects of the 6-dim terms in 2HDMEFT on the decay modes of the charged scalars. We calculate the production cross-section of the charged scalar following ref. [66] as it was recommended in ref. [67]. For $m_{H^\pm} > m_t$, the key production channel of H^\pm is through the process $pp \rightarrow H^\pm t$. The $H^\pm tb$ coupling multiplier depends on the value of $\tan \beta$ and the top and bottom quark masses. Following the $\tan \beta$ -dependence of $\sigma(H^\pm t)$ we rescale $\sigma(H^\pm t)$ at $\tan \beta = 30$ with the appropriate numerical factor to obtain the cross-sections at

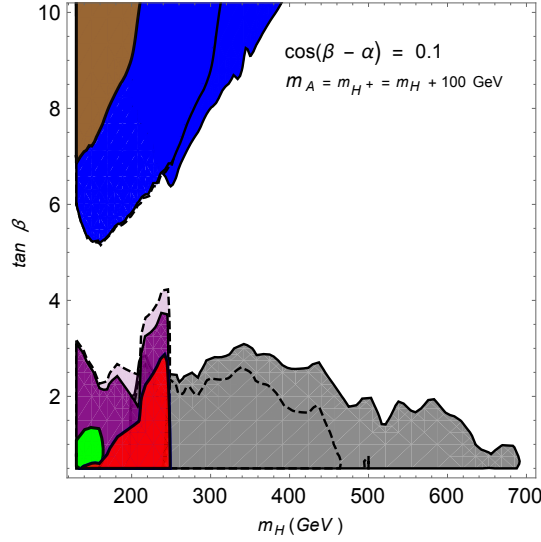


FIG. 6. The effect of $\varphi^4 D^2$ type of operators on the $m_H - \tan \beta$ plane in type-II 2HDM. The regions are excluded from $gg \rightarrow H \rightarrow WW$ (grey), $gg \rightarrow A \rightarrow ZH$ (purple), $gg \rightarrow A \rightarrow Zh$ (red), $gg \rightarrow A \rightarrow \tau\tau$ (green), $b\bar{b} \rightarrow A \rightarrow \tau\tau$ (brown), $b\bar{b} \rightarrow H \rightarrow \tau\tau$ (blue). In case of 2HDM EFT (dashed lines) the bounds from $A \rightarrow ZH$ and $H \rightarrow WW$ are different compared to 2HDM at tree-level (solid lines).

$\tan \beta = 1.5$ based on fig. 3 and 10 of ref. [66]. The traditional search channels of a charged Higgs boson considers the decay $H^+ \rightarrow \bar{\tau}\nu_\tau$ with a branching fraction of 100% [68]. Pertaining to different mass spectrum of 2HDM, the bounds on charged Higgs mass can be relaxed significantly [48]. The cascade decay channels with other Higgses as intermediate states can be interesting as well [48, 69]. In fig. 7 we have shown the contours of $\sigma(H^\pm t)\text{Br}(H^\pm \rightarrow hW^\pm)$ in **BP1** of 2HDM EFT for the 2HDM mass spectrum corresponding to cases **C1** and **C4** as discussed earlier. $\text{Br}(H^\pm \rightarrow HW^\pm)$ can change for the mass spectrum **C1** and can be followed from fig. 7(c). The decay channels consisting of SM fermions, such as $H^+ \rightarrow t\bar{b}, \bar{\tau}\nu_\tau, c\bar{s}$, etc., become quite important at higher values of $\tan \beta$. In fig. 7(d) we have shown the change in $\sigma \times \text{Br}$ with the decay channel $H^+ \rightarrow t\bar{b}$. Though the value of $\sigma \times \text{Br}$ in this channel is around one order smaller compared to the current LHC bound on such a process.

The coupling multiplier $\kappa_{H^\pm tb} \propto (m_t \tan \beta P_L + m_b \cot \beta P_R)$, and thus it reaches its minimum around $\tan \beta \sim 6 - 8$. Thus the production cross-section of H^\pm associated with a top quark becomes quite small for such values of $\tan \beta$. So we work only in scenarios when

$\tan\beta \sim 1$ and $\tan\beta \sim \mathcal{O}(10)$. We have not considered the case of $m_{H^\pm} \lesssim m_t$ when the key production mode of the charged scalar is $pp \rightarrow t\bar{t}$ with one of the tops in the final state decaying through $t \rightarrow bW^+$ and another one *via* $\bar{t} \rightarrow \bar{b}H^-$. For these values of m_{H^\pm} , bosonic decay channels of H^\pm , such as $H^\pm \rightarrow hW^\pm, HW^\pm$ are kinematically forbidden, unless one considers $m_H < m_h$, which is not the case for us.

In fig. 10 we have presented the values of $\sigma(H^\pm t)\text{Br}(H^\pm \rightarrow hW^\pm)$ in the alignment limit, in **BP1** of 2HDMEFT. The coupling $H^\pm hW^\mp$ vanishes at the alignment limit. But in presence of the 6-dim terms with the Wilson coefficients as in **BP1** of 2HDMEFT, the channel $H^\pm \rightarrow hW^\pm$ can become significant following the eqs. (4.2). It can be noticed that the cross-section in this channel attains significantly higher values for the cases **C1**, **C2** and **C3** compared to **C4**. For **C4**, the channel $H^\pm \rightarrow AW^\pm$ becomes kinematically accessible, thus lowering the value of $\text{Br}(H^\pm \rightarrow hW^\pm)$, leading to lesser cross-section compared to the other cases. For case **C3**, the cross-section can go up to ~ 25 fb for $m_{H^\pm} = 250$ GeV.

The couplings of $h(125)$ will be even more precisely measured in the future experiments. For instance, the coupling multipliers $\kappa_{h\gamma\gamma}$ and κ_{hWW} are to be measured with an accuracy of $\sim 5 - 7\%$ and $\sim 4 - 6\%$ respectively at HL-LHC with luminosity $\sim 3 \text{ ab}^{-1}$ [70]. It can push a 2HDM, especially the ones with type-II, -III and -IV Yukawa couplings, further close to $\cos(\beta - \alpha) = 0$. However, the contribution of dim-6 terms to the signal strengths of $h(125)$ do not decrease with the same scale. As it was also discussed in ref. [28], even at the exact limit $\cos(\beta - \alpha) = 0$, the effects of the dim-6 terms in masking the true alignment limit can be rather significant. Thus even at the limit when the couplings of $h(125)$ are exactly at par with the SM expectations, the heavier scalars are not decoupled from the rest of the particle spectrum. This remarkable feature can also be interpreted as the violation of the sum rules involving the couplings of the CP-even Higgses in 2HDM extended with dim-6 operators. In this paper, we have demonstrated several cases, where the cross-sections of certain decay channels of the heavier scalars are significant in the presence of 6-dim terms at $\cos(\beta - \alpha) = 0$. This leads to an interesting possibility of detecting the heavier scalars in these channels at HL-LHC, even if $h(125)$ exactly resembles the SM Higgs.

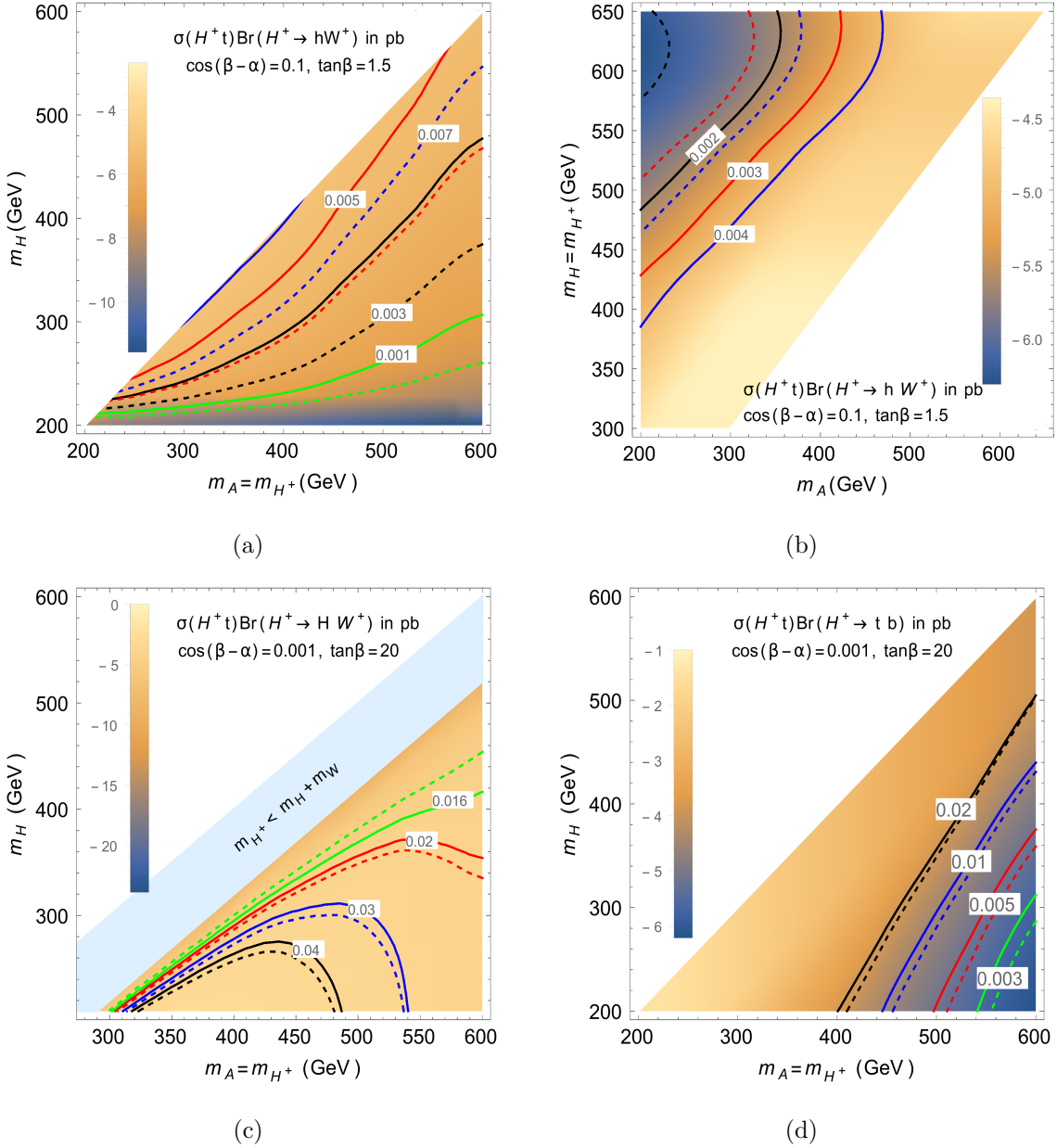


FIG. 7. The effect of 6-dim terms in type-II 2HDM on (a) $\sigma(H^\pm t) \text{Br}(H^\pm \rightarrow h W^\pm)$ for case **C1**, (b) $\sigma(H^\pm t) \text{Br}(H^\pm \rightarrow h W^\pm)$ for case **C4**, (c) $\sigma(H^\pm t) \text{Br}(H^\pm \rightarrow H W^\pm)$ for case **C1** and (d) $\sigma(H^\pm t) \text{Br}(H^\pm \rightarrow t \bar{b})$ for case **C1**. The solid and dotted lines correspond to the same values of $\sigma \times \text{Br}$ in 2HDM at tree-level and in **BP1** of 2HDMEFT respectively. The density plots depict the values of the corresponding $\sigma \times \text{Br}$ in the log-scale at LHC with $\sqrt{s} = 14$ TeV.

VI. SUMMARY AND DISCUSSIONS

In the context of the searches for new scalars at LHC, it is an interesting possibility that the exotic scalars in a 2HDM exist below the TeV scale, pertaining to the so-called ‘alignment-without-decoupling’ scenario. A study in 2HDMEFT becomes relevant in this case. Such an approach is appealing because it allows us to study the constraints in the 2HDM parameter space while remaining agnostic about any new physics beyond 2HDM. In this paper, we have confined our discussion to the bosonic operators of 2HDMEFT. The changes in the constraints on the masses of the exotic scalars of 2HDM are studied in the presence of 6-dim operators of type $\varphi^4 D^2$, because the other bosonic operators are quite constrained from electroweak precision tests.

We consider both degenerate and hierarchical mass spectra of the new scalars in this purpose and show the changes in the constraints for all four Yukawa types. The theoretical constraints, such as stability, perturbativity, and unitarity, as well as the measurement of the oblique parameters, restrict the mass differences of such scalars. In light of that one can narrow down four types of the mass spectrum in the hierarchical case. We notice that in a couple of such cases, dubbed as **C1** and **C2** in the text, the constraints on the $m_A - m_H$ plane can be significantly relaxed in the presence of certain 6-dim operators of type $\varphi^4 D^2$. For example, in case **C2** with $\cos(\beta - \alpha) = 0$, $\tan\beta = 1.5$ and type-I Yukawa coupling, the upper limit on m_H reduces to ~ 196 GeV in **BP1** of 2HDMEFT from ~ 300 GeV which is the case for 2HDM at tree-level. Such changes are always more pronounced for type-I and -IV 2HDM compared to type-II and -III.

At $\cos(\beta - \alpha) = 0$, processes such as $H \rightarrow ZZ$, $A \rightarrow Zh$, etc. vanish for 2HDM at the tree-level, which is not the case if dim-6 operators are present. A non-zero value for $\text{Br}(H \rightarrow WW)$ reduces the value of $\text{Br}(H \rightarrow b\bar{b})$, which brings down the cross-section for the process $pp \rightarrow A \rightarrow ZH(b\bar{b})$, thus relaxing the constraint on m_H . Such changes are not significant at higher values of $\tan\beta$ irrespective of the mass spectrum under consideration. This happens because the SM fermionic decay modes of the heavier scalars dominate for higher values of $\tan\beta$ and appearance of new bosonic decay channels cannot change the key decay channels involving SM fermions significantly. For the degenerate case we notice that, for our chosen benchmark scenario, the region excluded from the non-observation of H and

A becomes larger in 2HDMEFT compared to 2HDM at the tree-level. It is also seen, as it was discussed above, a certain mass range for $m_H(=m_A)$ is ruled out even for $\cos(\beta-\alpha)=0$ from processes like $H \rightarrow WW$, $A \rightarrow Zh$, which usually vanish in 2HDM at tree-level. We have also shown in fig. 7 the change in $\sigma \times \text{Br}$ for various decay channels of the charged scalar in 2HDMEFT compared to 2HDM at the tree-level at LHC with $\sqrt{s}=14$ TeV.

The key reason for the change in the constraints on 2HDM parameter space upon including dim-6 operators of type $\varphi^4 D^2$ lies in the redefinition of the CP-even Higgs fields, h , and H . This way the coupling multipliers involving the CP-even scalars are rescaled compared to 2HDM at the tree-level and lead to a change in the branching ratios of all the processes which involve h and H . It leads to the departure of the ‘true’ alignment limit from its tree-level 2HDM counterpart, *i.e.*, $\cos(\beta-\alpha)=0$. As the projected accuracy of the $h(125)$ coupling measurement at a future version of LHC, such as HL-LHC is at the level $\lesssim 5-6\%$, 2HDMs might get further pushed to the alignment limit. Thus, in the presence of dim-6 operators, even if the couplings of $h(125)$ turn out to be completely aligned with the SM Higgs, the heavier scalars in 2HDM with masses \lesssim TeV still do not decouple from the SM sector, *i.e.*, their discovery might still be viable. As mentioned earlier, some cascade-type decay channels of the heavier scalars vanish at the alignment limit in the tree-level 2HDM. It implies that the discovery of a new scalar in such a channel would perhaps rule out the alignment limit in a CP-conserving 2HDM. But if dim-6 operators are present, even if a new scalar is discovered in such channels, it will no longer rule out the alignment limit.

In case of the discovery of the new Higgs(es), the verification of the sum rules involving their coupling multipliers can provide useful information about the nature of the extended Higgs sector. In 2HDMEFT, the redefinition of the CP-even Higgs fields due to $\varphi^4 D^2$ operators also imply that the sum rules involving these scalars are modified in a certain way. We have discussed how the measurement of sum rules can help distinguishing between various options beyond a CP-even 2HDM.

If new scalars are discovered at the LHC in near future, the correlation of their signal strengths in different channels will be important to determine the exact nature of the underlying scalar sector. In this context, 2HDMEFT can be an efficient framework in quantifying the departure from tree-level 2HDM in various channels, providing an opportunity to narrow down the possible UV-complete scenarios.

VII. ACKNOWLEDGEMENTS

S.K. acknowledges T. Stefaniak for help regarding 2HDMC. This work is supported by the Department of Science and Technology, India *via* SERB grant EMR/2014/001177 and DST-DAAD grant INT/FRG/DAAD/P-22/2018.

Appendix A: Field redefinition

The redefinition of the physical CP-even neutral scalars in 2HDMEFT compared to 2HDM at the tree-level is given by eq. (4.2) along with,

$$\begin{aligned}
x_1 &= \frac{v^2}{f^2} \left(c_{H1} c_\beta^2 s_\alpha^2 + c_{H2} c_\alpha^2 s_\beta^2 + \frac{1}{8} c_{H1H2} s_{2\alpha} s_{2\beta} + c_{H12} (c_\alpha^2 c_\beta^2 + s_\alpha^2 s_\beta^2 - \frac{1}{4} s_{2\alpha} s_{2\beta}) \right. \\
&\quad \left. + c_{H1H12} c_\beta s_\alpha (s_\alpha s_\beta - \frac{1}{2} c_\alpha c_\beta) + c_{H2H12} c_\alpha s_\beta (c_\alpha c_\beta - \frac{1}{2} s_\alpha s_\beta) \right), \\
x_2 &= \frac{v^2}{f^2} \left(c_{H1} c_\beta^2 c_\alpha^2 + c_{H2} s_\alpha^2 s_\beta^2 + \frac{1}{8} c_{H1H2} s_{2\alpha} s_{2\beta} + c_{H12} (s_\alpha^2 c_\beta^2 + c_\alpha^2 s_\beta^2 - \frac{1}{4} s_{2\alpha} s_{2\beta}) \right. \\
&\quad \left. + c_{H1H12} c_\beta c_\alpha (c_\alpha s_\beta - \frac{1}{2} s_\alpha c_\beta) + c_{H2H12} s_\alpha s_\beta (s_\alpha c_\beta - \frac{1}{2} c_\alpha s_\beta) \right), \\
y &= \frac{v^2}{f^2} \left(\frac{1}{2} c_{H1} s_{2\alpha} c_\beta^2 - \frac{1}{2} c_{H2} s_{2\alpha} s_\beta^2 - \frac{1}{8} c_{H1H2} c_{2\alpha} s_{2\beta} - \frac{1}{2} c_{H12} (c_{2\beta} s_{2\alpha} + \frac{1}{2} c_{2\alpha} s_{2\beta}) \right. \\
&\quad \left. + \frac{1}{4} c_{H1H12} (s_{2\alpha} s_{2\beta} - c_{2\alpha} c_\beta^2) - \frac{1}{4} c_{H2H12} (s_{2\alpha} s_{2\beta} + c_{2\alpha} s_\beta^2) \right). \tag{A1}
\end{aligned}$$

Appendix B: Branching ratios in 2HDM vs. 2HDMEFT

The key branching ratios of H and A has been shown in fig. 8 with type-I and -II Yukawas for mass spectra **C1** and **C2**. When $m_{A(H)} \gtrsim 2m_t$, the channel $A(H) \rightarrow t\bar{t}$ becomes viable in all the cases. While showing the branching ratios for A we assume, $m_H = m_{H^\pm} = 130$ GeV and while showing the same for H we take, $m_A = m_H + 100$ GeV. For both these cases we take, $\cos(\beta - \alpha) = 0$ and $\tan\beta = 1.5$. $\text{Br}(A \rightarrow t\bar{t})$ attains values up to ~ 0.4 and ~ 0.19 for cases **C1** and **C2** respectively. In **C2**, $\text{Br}(A \rightarrow H^\pm W^\mp) \gtrsim 0.8$ for both type-I and -II 2HDM, whereas this process is absent for the case **C1**. This leads to a much lower values of $\text{Br}(A \rightarrow ZH)$ in **C2** compared to **C1**, which can be seen from figs. 8(a) and (b). Hence the non-observation of $A \rightarrow ZH$ rules out a larger region of parameter space in the case **C1** compared to **C2** even in tree-level 2HDM, which can be seen from figs. 1

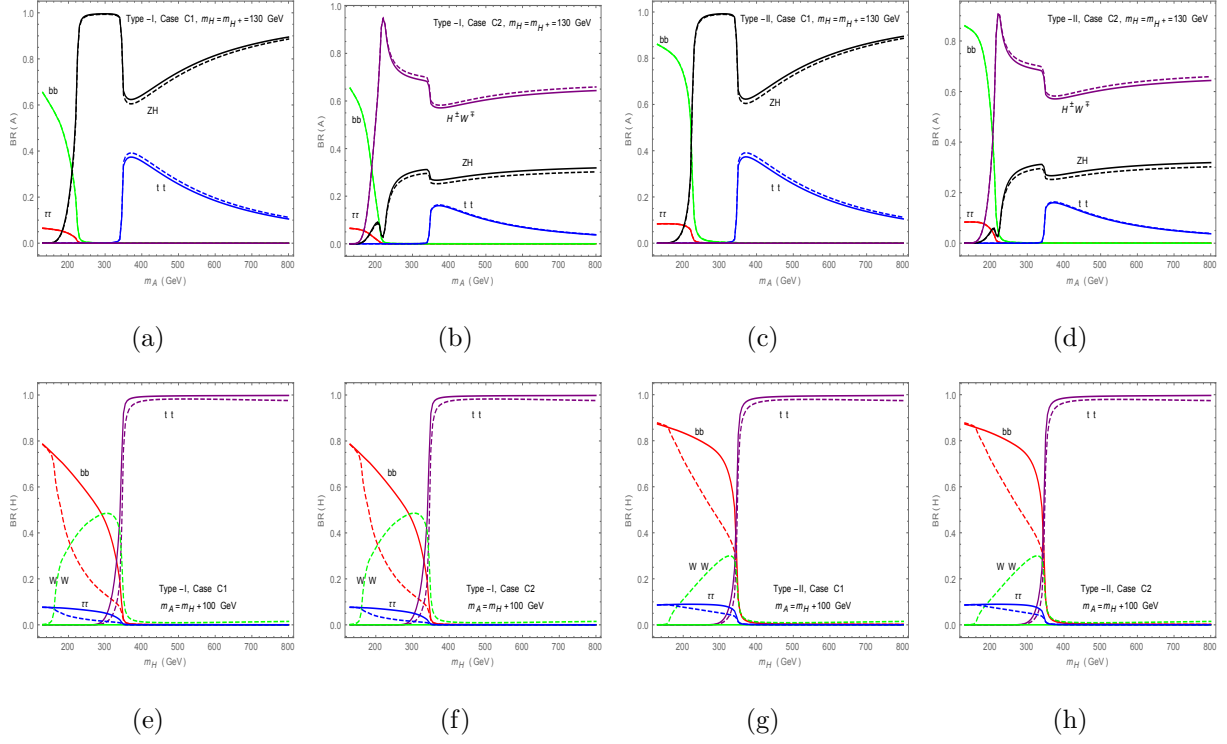


FIG. 8. The branching ratios of H and A in various channels which constrain the parameter space on the $\cos(\beta - \alpha) - m_A$ plane in the degenerate case.

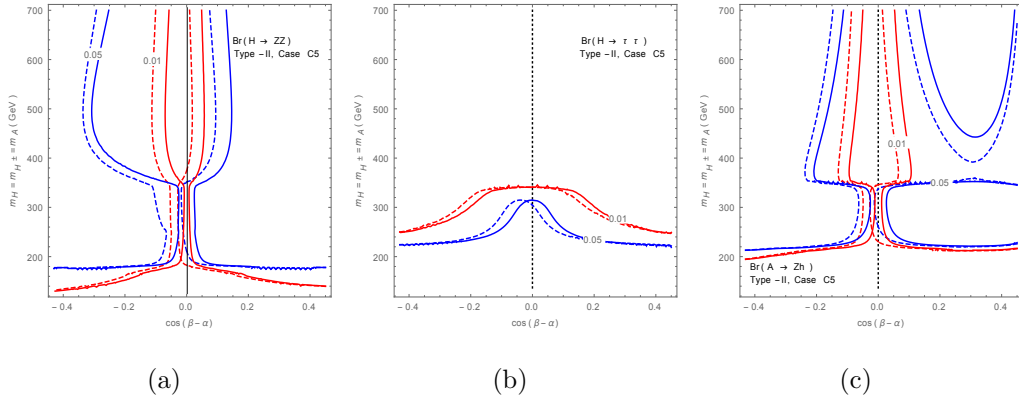


FIG. 9. The branching ratios of H and A in various channels which constrain the parameter space on the $\cos(\beta - \alpha) - m_A$ plane in the degenerate case **C5** for Type-II 2HDM. In all three figures, the solid and dashed lines represent the corresponding branching ratios in 2HDM at the tree-level and **BP1** of 2HDM EFT respectively.

and 2. From figs. 8(a) and (c) it can be seen that $\text{Br}(A \rightarrow \tau\bar{\tau})$ is larger for type-II 2HDM

compared to type-I. Thus the non-observation of $A \rightarrow \tau\bar{\tau}$ rules out a larger region for type-II 2HDM, as it can be seen from, for example, figs. 1(a) and (b). Figs. 8(e) and (f) show that $\text{Br}(H \rightarrow WW)$ can attain values up to ~ 0.5 for type-I 2HDM for both **C1** and **C2** at $\cos(\beta - \alpha) = 0$ in presence of 6-dim term, whereas it is vanishing in tree-level 2HDM. In contrary, as it can be seen from figs. 8(g) and (h), the corresponding value for type-II 2HDM can only go up to ~ 0.3 . However, the non-zero branching ratio of $H \rightarrow WW$ leads to a low value of $\text{Br}(H \rightarrow b\bar{b})$ and eventually a lower value of $A \rightarrow ZH(b\bar{b})$ compared to 2HDM at the tree-level, which explains the relaxed constraints on m_H as illustrated in fig. 1 and 2 on the $m_A - m_H$ plane. Such branching ratios in type-III and -IV 2HDM can also be followed from fig. 8 along with eq. (2.7), exploiting the patterns of couplings across Yukawa types. It can be seen that the constraints for type-I Yukawa resemble that for type-IV, whereas the constraints on type-II 2HDM are similar to that in type-III case.

Appendix C: $H^\pm \rightarrow hW^\pm$ cross-section at $\cos(\beta - \alpha) = 0$

The cross-sections in the channel $pp \rightarrow H^\pm \rightarrow hW^\pm$ for different hierarchical mass spectra have been presented in fig. 10. For $\cos(\beta - \alpha) = 0$, in 2HDM at the tree-level, such a process is absent. But in presence of the 6-dim operators, the cross-section for this process can go up to ~ 25 fb depending on the mass spectrum of 2HDM.

-
- [1] G. Aad *et al.* [ATLAS Collaboration], Phys. Lett. B **716** (2012) 1 doi:10.1016/j.physletb.2012.08.020 [arXiv:1207.7214 [hep-ex]].
 - [2] S. Chatrchyan *et al.* [CMS Collaboration], Phys. Lett. B **716** (2012) 30 doi:10.1016/j.physletb.2012.08.021 [arXiv:1207.7235 [hep-ex]].
 - [3] P. Fayet, Phys. Lett. B **64** (1976) 159, doi:10.1016/0370-2693(76)90319-1.
 - [4] J. Mrazek, A. Pomarol, R. Rattazzi, M. Redi, J. Serra and A. Wulzer, Nucl. Phys. B **853** (2011) 1 doi:10.1016/j.nuclphysb.2011.07.008 [arXiv:1105.5403 [hep-ph]].
 - [5] M. Schmaltz, D. Stolarski and J. Thaler, JHEP **1009** (2010) 018 doi:10.1007/JHEP09(2010)018 [arXiv:1006.1356 [hep-ph]].
 - [6] J. H. Yu, JHEP **1612** (2016) 143 doi:10.1007/JHEP12(2016)143 [arXiv:1608.05713 [hep-ph]].

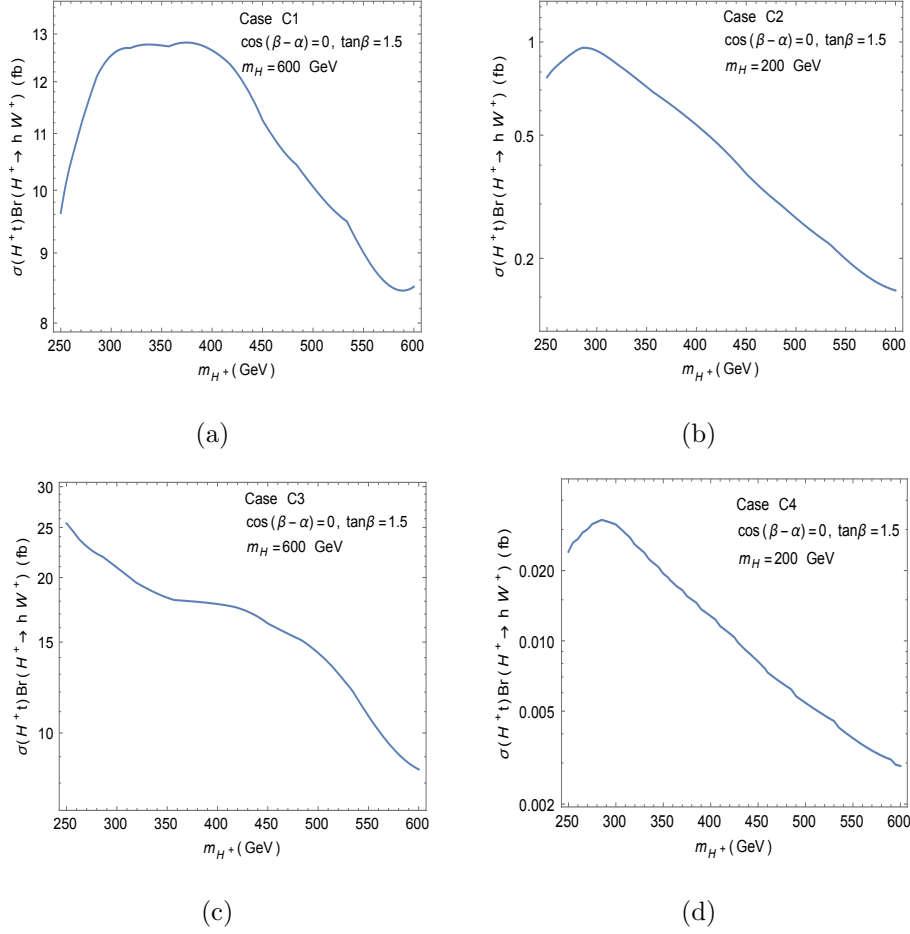


FIG. 10. $\sigma(H^\pm t)\text{Br}(H^\pm \rightarrow hW^\pm)$ in the alignment limit, in presence of the 6-dim terms at LHC with $\sqrt{s} = 14$ TeV in type-II 2HDM.

- [7] M. Trodden, Rev. Mod. Phys. **71** (1999) 1463 doi:10.1103/RevModPhys.71.1463 [hep-ph/9803479].
- [8] A. Crivellin, C. Greub and A. Kokulu, Phys. Rev. D **86** (2012) 054014 doi:10.1103/PhysRevD.86.054014 [arXiv:1206.2634 [hep-ph]].
- [9] E. Ma, Phys. Rev. D **73** (2006) 077301 doi:10.1103/PhysRevD.73.077301 [hep-ph/0601225].
- [10] R. Barbieri, L. J. Hall and V. S. Rychkov, Phys. Rev. D **74** (2006) 015007 doi:10.1103/PhysRevD.74.015007 [hep-ph/0603188].
- [11] H. Georgi and D. V. Nanopoulos, Phys. Lett. B **82** (1979) 95, doi:10.1016/0370-2693(79)90433-7.

- [12] J. F. Gunion and H. E. Haber, Phys. Rev. D **67** (2003) 075019 doi:10.1103/PhysRevD.67.075019 [hep-ph/0207010].
- [13] A. Delgado, G. Nardini and M. Quiros, JHEP **1307** (2013) 054 doi:10.1007/JHEP07(2013)054 [arXiv:1303.0800 [hep-ph]].
- [14] M. Carena, I. Low, N. R. Shah and C. E. M. Wagner, JHEP **1404** (2014) 015 doi:10.1007/JHEP04(2014)015 [arXiv:1310.2248 [hep-ph]].
- [15] J. Bernon, J. F. Gunion, H. E. Haber, Y. Jiang and S. Kraml, Phys. Rev. D **92** (2015) no.7, 075004 doi:10.1103/PhysRevD.92.075004 [arXiv:1507.00933 [hep-ph]].
- [16] J. Bernon, J. F. Gunion, H. E. Haber, Y. Jiang and S. Kraml, Phys. Rev. D **93** (2016) no.3, 035027 doi:10.1103/PhysRevD.93.035027 [arXiv:1511.03682 [hep-ph]].
- [17] H. E. Haber, arXiv:1401.0152 [hep-ph].
- [18] H. E. Haber, arXiv:1805.05754 [hep-ph].
- [19] B. Grzadkowski, H. E. Haber, O. M. Ogreid and P. Osland, arXiv:1808.01472 [hep-ph].
- [20] J. L. Diaz-Cruz, J. Hernandez-Sanchez and J. J. Toscano, Phys. Lett. B **512** (2001) 339 doi:10.1016/S0370-2693(01)00703-1 [hep-ph/0106001].
- [21] A. Crivellin, M. Ghezzi and M. Procura, JHEP **1609** (2016) 160 doi:10.1007/JHEP09(2016)160 [arXiv:1608.00975 [hep-ph]].
- [22] S. Karmakar and S. Rakshit, JHEP **1710** (2017) 048 doi:10.1007/JHEP10(2017)048 [arXiv:1707.00716 [hep-ph]].
- [23] M. Chala, G. Durieux, C. Grojean, L. de Lima and O. Matsedonskyi, JHEP **1706** (2017) 088 doi:10.1007/JHEP06(2017)088 [arXiv:1703.10624 [hep-ph]].
- [24] Y. Kikuta, Y. Okada and Y. Yamamoto, Phys. Rev. D **85** (2012) 075021 doi:10.1103/PhysRevD.85.075021 [arXiv:1111.2120 [hep-ph]].
- [25] Y. Kikuta and Y. Yamamoto, Eur. Phys. J. C **76** (2016) no.5, 297 doi:10.1140/epjc/s10052-016-4128-3 [arXiv:1510.05540 [hep-ph]].
- [26] N. Fonseca, R. Zukanovich Funchal, A. Lessa and L. Lopez-Honorez, JHEP **1506** (2015) 154 doi:10.1007/JHEP06(2015)154 [arXiv:1501.05957 [hep-ph]].
- [27] A. Banerjee, G. Bhattacharyya and N. Kumar, arXiv:1901.01725 [hep-ph].
- [28] S. Karmakar and S. Rakshit, JHEP **1809** (2018) 142 doi:10.1007/JHEP09(2018)142 [arXiv:1802.03366 [hep-ph]].

- [29] I. F. Ginzburg and M. Krawczyk, Phys. Rev. D **72** (2005) 115013 doi:10.1103/PhysRevD.72.115013 [hep-ph/0408011].
- [30] A. W. El Kaffas, P. Osland and O. M. OGREID, Nonlin. Phenom. Complex Syst. **10** (2007) 347 [hep-ph/0702097 [HEP-PH]].
- [31] S. L. Glashow and S. Weinberg, Phys. Rev. D **15** (1977) 1958, doi:10.1103/PhysRevD.15.1958.
- [32] E. A. Paschos, Phys. Rev. D **15** (1977) 1966. doi:10.1103/PhysRevD.15.1966.
- [33] P. S. Bhupal Dev and A. Pilaftsis, JHEP **1412** (2014) 024 Erratum: [JHEP **1511** (2015) 147] doi:10.1007/JHEP11(2015)147, 10.1007/JHEP12(2014)024 [arXiv:1408.3405 [hep-ph]].
- [34] A. Pilaftsis, Phys. Rev. D **93** (2016) no.7, 075012 doi:10.1103/PhysRevD.93.075012 [arXiv:1602.02017 [hep-ph]].
- [35] D. Das, U. K. Dey and P. B. Pal, Phys. Rev. D **96** (2017) no.3, 031701 doi:10.1103/PhysRevD.96.031701 [arXiv:1705.07784 [hep-ph]].
- [36] K. Benakli, Y. Chen and G. Lafforgue-Marmet, arXiv:1811.08435 [hep-ph].
- [37] S. Pramanick and A. Raychaudhuri, JHEP **1801** (2018) 011 doi:10.1007/JHEP01(2018)011 [arXiv:1710.04433 [hep-ph]].
- [38] N. Craig, J. Galloway and S. Thomas, arXiv:1305.2424 [hep-ph].
- [39] P. M. Ferreira, R. Guedes, J. F. Gunion, H. E. Haber, M. O. P. Sampaio and R. Santos, arXiv:1410.1926 [hep-ph].
- [40] T. Modak, J. C. Romao, S. Sadhukhan, J. P. Silva and R. Srivastava, Phys. Rev. D **94** (2016) no.7, 075017 doi:10.1103/PhysRevD.94.075017 [arXiv:1607.07876 [hep-ph]].
- [41] P. M. Ferreira, J. F. Gunion, H. E. Haber and R. Santos, Phys. Rev. D **89** (2014) no.11, 115003 doi:10.1103/PhysRevD.89.115003 [arXiv:1403.4736 [hep-ph]].
- [42] G. C. Dorsch, S. J. Huber, K. Mimasu and J. M. No, Phys. Rev. D **93** (2016) no.11, 115033 doi:10.1103/PhysRevD.93.115033 [arXiv:1601.04545 [hep-ph]].
- [43] G. C. Dorsch, S. J. Huber, K. Mimasu and J. M. No, Phys. Rev. Lett. **113** (2014) no.21, 211802 doi:10.1103/PhysRevLett.113.211802 [arXiv:1405.5537 [hep-ph]].
- [44] G. C. Dorsch, S. J. Huber and J. M. No, JHEP **1310** (2013) 029 doi:10.1007/JHEP10(2013)029 [arXiv:1305.6610 [hep-ph]].
- [45] C. Gao, M. A. Luty, M. Mulhearn, N. A. Neill and Z. Wang, Phys. Rev. D **97** (2018) no.7, 075040 doi:10.1103/PhysRevD.97.075040 [arXiv:1604.03108 [hep-ph]].

- [46] M. Bauer, M. Carena and K. Gemmler, JHEP **1511** (2015) 016 doi:10.1007/JHEP11(2015)016 [arXiv:1506.01719 [hep-ph]].
- [47] F. Kling, A. Pyarelal and S. Su, JHEP **1511** (2015) 051 doi:10.1007/JHEP11(2015)051 [arXiv:1504.06624 [hep-ph]].
- [48] B. Coleppa, F. Kling and S. Su, JHEP **1412** (2014) 148 doi:10.1007/JHEP12(2014)148 [arXiv:1408.4119 [hep-ph]].
- [49] F. Kling, J. M. No and S. Su, JHEP **1609** (2016) 093 doi:10.1007/JHEP09(2016)093 [arXiv:1604.01406 [hep-ph]].
- [50] A. Adhikary, S. Banerjee, R. K. Barman and B. Bhattacharjee, arXiv:1812.05640 [hep-ph].
- [51] F. Kling, H. Li, A. Pyarelal, H. Song and S. Su, arXiv:1812.01633 [hep-ph].
- [52] W. Grimus, L. Lavoura, O. M. Ogreid and P. Osland, J. Phys. G **35** (2008) 075001 doi:10.1088/0954-3899/35/7/075001 [arXiv:0711.4022 [hep-ph]].
- [53] W. Grimus, L. Lavoura, O. M. Ogreid and P. Osland, Nucl. Phys. B **801** (2008) 81 doi:10.1016/j.nuclphysb.2008.04.019 [arXiv:0802.4353 [hep-ph]].
- [54] H. E. Haber and D. O’Neil, Phys. Rev. D **83** (2011) 055017 doi:10.1103/PhysRevD.83.055017 [arXiv:1011.6188 [hep-ph]].
- [55] G. Abbiendi *et al.* [ALEPH and DELPHI and L3 and OPAL and LEP Collaborations], Eur. Phys. J. C **73** (2013) 2463 doi:10.1140/epjc/s10052-013-2463-1 [arXiv:1301.6065 [hep-ex]].
- [56] S. Schael *et al.* [ALEPH and DELPHI and L3 and OPAL Collaborations and LEP Working Group for Higgs Boson Searches], Eur. Phys. J. C **47** (2006) 547 doi:10.1140/epjc/s2006-02569-7 [hep-ex/0602042].
- [57] F. Mahmoudi and O. Stål, Phys. Rev. D **81** (2010) 035016 doi:10.1103/PhysRevD.81.035016 [arXiv:0907.1791 [hep-ph]].
- [58] O. Eberhardt, U. Nierste and M. Wiebusch, JHEP **1307** (2013) 118 doi:10.1007/JHEP07(2013)118 [arXiv:1305.1649 [hep-ph]].
- [59] T. Han, T. Li, S. Su and L. T. Wang, JHEP **1311** (2013) 053 doi:10.1007/JHEP11(2013)053 [arXiv:1306.3229 [hep-ph]].
- [60] The ATLAS collaboration [ATLAS Collaboration], ATLAS-CONF-2017-055.
- [61] A. M. Sirunyan *et al.* [CMS Collaboration], arXiv:1806.00408 [hep-ex].
- [62] The ATLAS collaboration, ATLAS-CONF-2016-015.

- [63] The ATLAS collaboration [ATLAS Collaboration], ATLAS-CONF-2017-050.
- [64] D. Eriksson, J. Rathsman and O. Stål, Comput. Phys. Commun. **181** (2010) 189
doi:10.1016/j.cpc.2009.09.011 [arXiv:0902.0851 [hep-ph]].
- [65] R. V. Harlander, S. Liebler and H. Mantler, Comput. Phys. Commun. **184** (2013) 1605
doi:10.1016/j.cpc.2013.02.006 [arXiv:1212.3249 [hep-ph]].
- [66] M. Flechl, R. Klees, M. Kramer, M. Spira and M. Ubiali, Phys. Rev. D **91** (2015) no.7, 075015
doi:10.1103/PhysRevD.91.075015 [arXiv:1409.5615 [hep-ph]].
- [67] S. Heinemeyer *et al.* [LHC Higgs Cross Section Working Group], doi:10.5170/CERN-2013-004
arXiv:1307.1347 [hep-ph].
- [68] CMS Collaboration [CMS Collaboration], CMS-PAS-HIG-14-020.
- [69] A. Arhrib, R. Benbrik and S. Moretti, Eur. Phys. J. C **77** (2017) no.9, 621
doi:10.1140/epjc/s10052-017-5197-7 [arXiv:1607.02402 [hep-ph]].
- [70] The ATLAS collaboration [ATLAS Collaboration], ATL-PHYS-PUB-2018-054.